Journal of Hydrology 559 (2018) 327–346

Contents lists available at ScienceDirect

Journal of Hydrology

journal homepage: www.elsevier.com/locate/jhydrol

Research papers

Regional variation of flow duration curves in the eastern United States: Process-based analyses of the interaction between climate and landscape properties

Wafa Chouaib [a,*], Peter V. Caldwell [b], Younes Alila [c]

[a] Department of Forest Resources Management 2404, University of British Columbia, 2424 Main Mall, Vancouver, BC V6T 1Z4, Canada
[b] USDA Forest Service, Southern Research Station, Center for Forest Watershed Research, Coweeta Hydrologic Lab, 3160 Coweeta Lab Road, Otto, NC 28734, USA
[c] Department of Forest Resources Management 2030, 2424 Main Mall, Vancouver, BC V6T 1Z4, Canada

ARTICLE INFO

Article history:
Received 21 May 2017
Received in revised form 29 November 2017
Accepted 15 January 2018
Available online 3 February 2018
This manuscript was handled by A. Bardossy, Editor-in-Chief, with the assistance of Roger Moussa, Associate Editor

Keywords:
Flow duration curve
Regional variation
Catchment filter
Precipitation
Topographic index
Runoff processes

ABSTRACT

This paper advances the physical understanding of the flow duration curve (FDC) regional variation. It provides a process-based analysis of the interaction between climate and landscape properties to explain disparities in FDC shapes. We used (i) long term measured flow and precipitation data over 73 catchments from the eastern US. (ii) We calibrated the Sacramento model (SAC-SMA) to simulate soil moisture and flow components FDCs. The catchments classification based on storm characteristics pointed to the effect of catchments landscape properties on the precipitation variability and consequently on the FDC shapes. The landscape properties effect was pronounce such that low value of the slope of FDC (SFDC)—hinting at limited flow variability—were present in regions of high precipitation variability. Whereas, in regions with low precipitation variability the SFDCs were of larger values. The topographic index distribution, at the catchment scale, indicated that saturation excess overland flow mitigated the flow variability under conditions of low elevations with large soil moisture storage capacity and high infiltration rates. The SFDCs increased due to the predominant subsurface stormflow in catchments at high elevations with limited soil moisture storage capacity and low infiltration rates. Our analyses also highlighted the major role of soil infiltration rates on the FDC despite the impact of the predominant runoff generation mechanism and catchment elevation. In conditions of slow infiltration rates in soils of large moisture storage capacity (at low elevations) and predominant saturation excess, the SFDCs were of larger values. On the other hand, the SFDCs decreased in catchments of prevalent subsurface stormflow and poorly drained soils of small soil moisture storage capacity. The analysis of the flow components FDCs demonstrated that the interflow contribution to the response was the higher in catchments with large value of slope of the FDC. The surface flow FDC was the most affected by the precipitation as it tracked the precipitation duration curve (PDC). In catchments with low SFDCs, this became less applicable as surface flow FDC diverged from PDC at the upper tail (> 40% of the flow percentile). The interflow and baseflow FDCs illustrated most the filtering effect on the precipitation. The process understanding we achieved in this study is key for flow simulation and assessment in addition to future works focusing on process-based FDC predictions.

1. Introduction

One of the most fundamental problems facing the hydrological community over the last several decades has been the lack of comprehensive understanding about the relative contributions of climatic and watershed characteristics on streamflow and the shape of flow duration curves (FDCs) (Yokoo and Sivapalan, 2011). A flow duration curve (FDC) graphically illustrates the percentage of time (duration) that streamflow exceeds a given value over a historical period for a particular river basin (e.g., Vogel and Fennessey, 1994). If the streamflow is assumed to be a random variable, the FDC may also be viewed as the complement of the cumulative distribution function of the flow (CDF) (e.g., Vogel and Fennessey, 1994; LeBoutillier and Waylen, 1993). The FDC representation is relevant in many hydrologic applications including reservoir and lake sedimentation studies, stream flow assessments, hydropower feasibility analysis, water quality management, waste load alloca-

* Corresponding author.
E-mail addresses: wafa.chouaib@alumni.ubc.ca, chouaiebwafa@gmail.com (W. Chouaib), pcaldwell02@fs.fed.us (P.V. Caldwell), younes.alila@ubc.ca (Y. Alila).

https://doi.org/10.1016/j.jhydrol.2018.01.037
0022-1694/

tion, and water resource allocation (Vogel and Fennessey, 1994; Vogel and Fennessey, 1995). Over the past several decades, FDCs have been analyzed using a graphical representation (Ward and Robinson, 1990) or stochastic models in order to fit the appropriate statistical distribution to empirical FDCs (Cigizoglu and Bayazit, 2000; Sugiyama et al., 2003; Castellarin, 2004a; Iacobellis, 2008). These studies helped the hydrologic community in issues related to the prediction of the FDC without explicitly advancing the physical understanding of the FDC controls. Most often, the prediction studies at the ungauged catchments related the physiographic characteristics to the statistical moments of the FDC probability distributions (LeBoutillier and Waylen, 1993; Singh and Mishra, 2001; Claps and Fiorentino, 1997; Croker et al., 2003; Smakhtin and Hughes, 1997; Fennessey and Vogel, 1990; Castellarin et al., 2004b). This approach does not provide understanding of the FDC controls. Few researches dealing with the prediction at ungauged catchments provided implicit understanding of the FDC controls. For instance, Musiake et al. (1975) emphasized the prevalent effect of the geology structure on characterizing the baseflow after they classified the study catchments (small to medium sized) into physiographic classes and analyzed the baseflow data transfer between catchments of the same class. Sefton and Howarth (1998) derived the parameters' values of a rainfall-runoff model from relationships with the morphometric and physiographic characteristics over 60 catchments in UK. These relationships indicated, through sensitivity analyses of the parameters, the collective effect of the landscape characteristics (soil, land use, slope and elevation) on the FDC shapes. The effect of the geology structure and the landscape characteristics remained indicative and required a detailed physical and quantitative analyses. One of the rare studies that addressed thoroughly the effect of the vegetation types on the shape of the FDCs is Burt and Swank (1992). The study demonstrated that fertilized grass and the forest cover controlled similarly the discharge levels for all the frequency classes. The existing literature can be used as base for our study towards a more comprehensive understanding of the FDC controls.

Another category of studies analyzed the FDCs from the perspective of runoff processes using stochastic modeling (Botter et al., 2007a; Muneepeerakul et al., 2010a,b); Botter et al., 2009). The investigations contributed to advance the understanding of the FDC controls. Botter et al. (2007a) derived the slow-flow component FDC (baseflow) through analysis of the soil moisture dynamics and the statistical properties of the precipitation. Subsequently, Botter et al. (2009) included non-linearity in the subsurface storage discharge relationship, and Muneepeerakul et al. (2010a,b) extended the same model to include a fast-flow component (surface flow). The ability of the model to reproduce observed FDCs has been tested in small to medium sized catchments in both the US and Europe (Botter et al., 2007b; Ceola et al., 2010; Botter, 2010). However, this stochastic dynamic model builds on assumptions about precipitation (i.e., non-random events in Poisson rainfall arrival) and could only be applied seasonally with constant parameter values for each season (Botter et al., 2007a,b). Therefore, overcoming the limitations of the stochastic dynamic framework reviewed above would further help in revealing the climatic and landscape controls of the FDCs.

In the continental US, a recent series of empirical studies analyzed the pattern of change of the FDCs in catchments from all the US (Cheng et al., 2012; Coopersmith et al., 2012; Ye et al., 2012). The study catchments had diverse climate and landscape properties. At a first stage, Cheng et al. (2012) analyzed the FDC shape from the correlation of their statistical moments, when fitted to a gamma distribution, with first-order catchment characteristics (i.e., baseflow index, maximum daily precipitation, and a fraction of non-rainy days). Subsequently, in a study by Coopersmith et al. (2012), the study catchments were classified into climate clusters based on climate signatures (i.e., precipitation seasonality index, seasonality index of the precipitation, and day of peak precipitation). The climate clusters helped Yaeger et al. (2012) to investigate the spatial pattern of FDCs using the process controls of the seasonal flow response in the US; namely the aridity, the snowmelt and the phenology. These processes were determined by the combined modeling and empirical water balance study of Ye et al. (2012). However, the large extent of the study area (i.e., the entire continental US) did not reveal sufficient detail about the climatic and landscape controls of FDCs. The characteristics of climate seasonality, aridity, and phenology that influenced the average seasonal flow response in Ye et al. (2012) were not sufficient to explain the diversity of FDC shapes across the continental US (Yaeger et al., 2012).

A study by Yokoo and Sivapalan (2011) examined the shapes of FDCs under several theoretical combinations of landscape properties with climate. This study developed a conceptual framework to predict FDCs using a runoff process-based approach. The framework considered the FDC as constructed from precipitation variability that cascades through the catchment system and gets exposed to landscapes in order to generate runoff under its respective process controls (Cheng et al., 2012). This conceptual framework provided some understanding, but it required further analyses and testing using observed data (Yokoo and Sivapalan, 2011). Nonetheless, it can also serve as guidance for investigations focusing on the study of FDC controls.

Even with previous research regarding the factors that control the shapes of the FDCs, we remain far from understanding the physical mechanisms behind the regional variation of FDC. The need for a process-based understanding motivated the research goals of this study. Therefore, here we propose to analyze the regional variation of FDCs in the eastern US to advance our current physical understanding about FDC controls. The eastern US has considerable variability in landscape (i.e., mountains and plains) and climate. In particular, the mountainous Appalachian region has historically been prone to flooding caused by late winter and early spring rains as well as snowmelt, summer cloudbursts, and remnants of tropical systems (Perry and Combs, 1998; Perry et al., 2001; Hicks et al., 2005). The following questions guided our research: 1) If the regional variation of FDCs is controlled by the interaction of climate and landscape properties, then to what extent is the diversity in the shapes of FDCs explained by each of the controls? and 2) In response to their effect, what is the aspect of the runoff processes that govern the regional variation of FDCs?

We developed a number of methods to answer our research questions. In this paper, we used rainfall-runoff data from 73 catchments across the eastern US, and through a combination of data analysis and conceptual rainfall-runoff modeling, we analyzed the diversity in precipitation and in storms of the study catchments. Then, we developed a framework to characterize differences and similarities in landscape properties to measure their interaction with precipitation to affect the FDC. We elucidated the effect of FDC controls on the flow components and runoff processes, and we investigated the distributions of topographic indexes at the catchment level.

Our overall goal was to provide a detailed analysis of the climate and landscape properties in the region of interest and to advance the process understanding of the physical relationships between the shapes of FDCs and the effect of climate and landscape properties.

2. Dataset and study area

2.1. Dataset

The catchments used in this study are part of the database developed for the Model Parameter Estimation Experiment

(MOPEX) (Duan et al., 2006; Schaake et al., 2006). The database contains historical hydro-meteorological data and land surface characteristics for many hydrological basins in the US and in other countries (Duan et al., 2006). MOPEX research has been driven by a series of international workshops that brought together interested hydrologists and modellers to exchange knowledge and experience in developing and applying model parameter estimation techniques. With its focus on parameter estimation, MOPEX plays a major role in the context of international initiatives such as Prediction in Ungauged Basins (PUB) (Hrachowitz et al., 2013). We extracted all the data of catchments located within the study area from the MOPEX database. We chose the MOPEX because it has relatively long record length (50 years on average) and it has been used repeatedly in several researches in the U.S (Koren et al., 2003; Cheng et al., 2012; Coopersmith et al., 2012; Ye et al., 2012; Berghuijs et al., 2014, 2016).

The database is freely available and was retrieved from the following website: www.nws.noaa.gov/oh/mopex/mo_datasets.htm.

Air temperature, potential evapotranspiration (PET), and streamflow are all available with a daily time step. Precipitation data is representative of the catchment average and is available at both daily and hourly time steps. In this study we use the hourly and daily precipitation, as well as the daily flow and daily PET. The record length ranges from 1948 to 2000. The MOPEX catchments are considered to be associated with a natural flow regime with limited human influence (Schaake et al., 2006).

2.2. Study area characteristics

We studied the spatial pattern of FDCs using 73 MOPEX catchments from the eastern US. The mean annual precipitation (MAP) in the study catchments varies between 702 mm and 2072 mm (see Appendix, Table 1). The catchments have a humid climate. The aridity index (the ratio of the MAP by the potential evapotranspiration) is rather low according to Coopersmith et al. (2012) (see Appendix, Table 1 where the catchments are sorted according to their site code). The catchment size ranged from 67 km^2 to 8052 km^2, as shown in Fig. 1a and Table 1 (Appendix). Around 20% of the catchments have sizes above 4000 km^2. The catchments are mainly forested with some proportions of agricultural lands and limited influence of urban areas (see Appendix, Table 1). The catchments' runoff ratio —that is the annual runoff by the annual precipitation ratio— has a minimum of 0.33, a maximum of 0.64, and a median of 0.44 (see Appendix, Table 1). Perennial snow cover is absent for most catchments and does not exceed 3% of the surface area for individual catchments (Berghuijs et al., 2014). The precipitation in the eastern US is of low seasonality (Fig. 1(b)) (Coopersmith et al., 2012; Sawicz et al., 2011). The mean monthly precipitation has limited fluctuation through seasons, whereas storm characteristics—in particular storm intensity—have systematic seasonal variation (Hershfield, 1961). Orographic thunderstorms are common in the Appalachian Mountains and produce large rainfall accumulations that may exceed 600 mm for 6 h storms (Erskine, 1951; Eisenlohr, 1952; Miller, 1990; Smith et al., 1996). At the headwater scale, orographic thunderstorms lead to large floods that may exceed the 500-year return period such as the event of November 1985 in Central Appalachian (see Miller, 1990).

The Appalachian Mountains create a contrast in elevations as shown by the Digital Elevation Model (DEM) in Fig. 2. Catchments with low relief are mainly located in the eastern coast and in the state of Georgia, while the interior catchments have higher relief. The maximum elevation across the region is 2029 m above sea level (m.a.s.l), and the minimum is -93 m.a.s.l. (Fig. 2). This area of low elevation refers to a wetland in Florida that lies below sea level. In this study, we do not describe the detailed geomorphology and geology descriptors (i.e., impermeable areas, spring horizon, intermittent streams) covering such a large region because of limited availability.

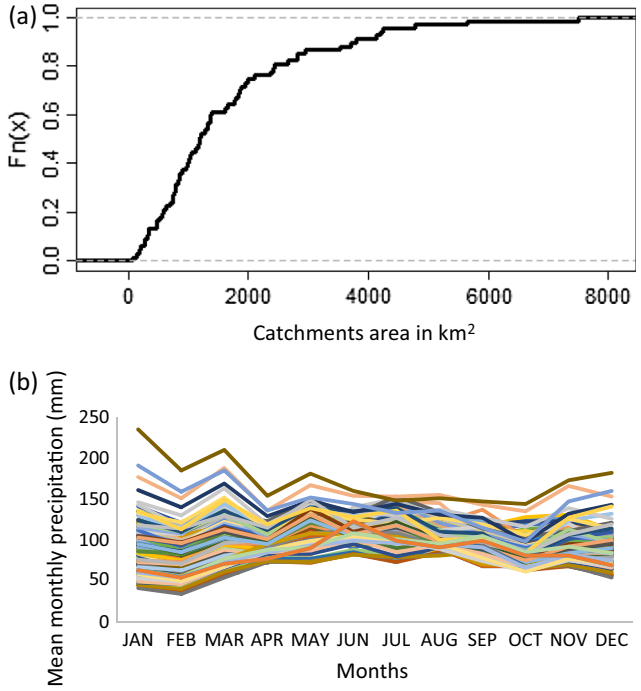

Fig. 1. (a) Catchment size distribution, (b) mean monthly precipitation (mm).

The variation in soil texture and structure across the study region affects the soil hydrologic properties and so the flow response (Wood et al., 1984). Fig. 2 illustrates the spatial pattern of the main hydrologic groups HGB (soil with medium infiltration rate) and HGC (soil with slow infiltration rate) (Wood et al., 1984); note that there is a gradual decrease of HGB soils from the southern to northern regions. In mid-latitudes, the soil is a combination of HGB and HGC, while in northeast it becomes predominantly HGC.

3. Methods

Our analysis of the regional variation of FDCs covered two main dimensions: (i) the study of FDC shapes in the context of landscape properties acting as a filter for precipitation at the catchment scale; and (ii) detailed analyses of the spatial pattern of the FDCs using flow components and runoff-generation mechanisms.

Prior to the FDC analyses, we grouped the study catchments into clusters of homogeneous storm characteristics in order to control for climate and isolate the effect of landscape properties on the regional variation of FDCs. We diagnosed the seasonality of storm characteristics in each catchment. This has been achieved by storm separation of hourly precipitation (see Section 3.1 below). We analyzed the slope of the FDCs (SFDCs) and their regional variation (i.e., the slope of the FDC is surrogate of the flow variability (Sawicz et al., 2011), see Section 3.4 of this manuscript for more details on how the slope of the FDC is calculated and defined). We defined categories of flow variability across study catchments based on the average value of SFDCs. Then, we investigated the differences in FDCs from the interaction of catchment filter with precipitation variability. We assessed the effect of catchment filter from the spatial pattern of FDCs and the precipitation duration curves (PDCs) using as guidance the conceptual framework of Yokoo and Sivapalan (2011). The slopes of the precipitation duration curve (PDC) are considered a surrogate of precipitation

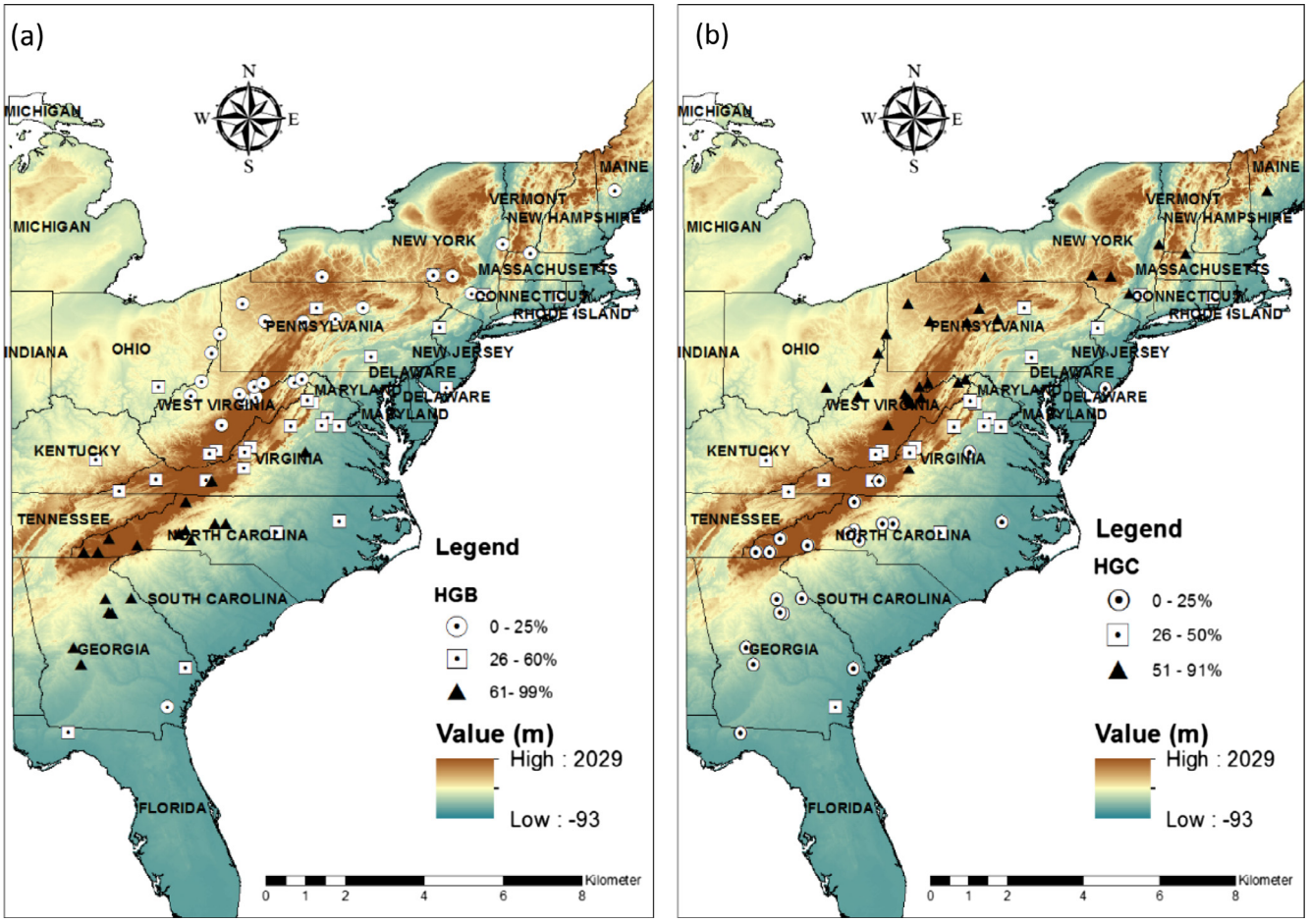

Fig. 2. DEM and spatial pattern of soil hydrologic groups (a) HGB and (c) HGC.

variability. The catchment filter effect on the precipitation collectively represent the impact of the landscape properties (i.e., soil hydrologic properties, surface topography, and vegetation type) and the geology structure. The limited availability of detailed descriptors of the vegetation (i.e., age, density, species) and the geology suggests we focus, in combination to the storm characteristics, on the impact of the landscape properties and the soil moisture storage capacity (SMSC). We calibrated the SAC-SMA model to predict the daily soil moisture and estimate the SMSC at the catchment scale. The SAC-SMA model has been applied worldwide and particularly in the different hydro-climate regimes of the United States (Koren et al., 2003). It allows for more detailed flow simulations by separating flow into runoff components, namely, the direct runoff, surface runoff, interflow, and baseflow (van Werkhoven et al., 2008; Burnash, 1995).

We utilised the flow components provided by SAC-SMA simulations to meet the second dimension of our research goal. We also determined the predominant runoff generation mechanisms after we investigated the topographic index (TI) distribution at the catchment scale. These process-based investigations explained the physical reasons for the regional variation of the FDCs. At this level, we reassessed the effect of the catchment filter on precipitation (PDC) to determine the flow component FDC that is directly affected by the precipitation variability. Fig. 3 summarizes the several steps of our study.

3.1. Storm separation

We obtained hourly rainfall data from the MOPEX database that is available for each study catchment. We separated the hourly rainfall into storm and inter-storm periods using an automated objective algorithm. The separation criterion is a specified minimum dry period between consecutive events equal to 6 h (Erskine, 1951; Eisenlohr, 1952; Miller, 1990; Smith et al., 1996), which is similar to what other researchers have adopted: Hershfield (1961) and Huff (1967) used 6 h; Koutsoyiannis and Foufoula-Georgiou (1993) used 7 h. Robinson and Sivapalan (1997) used 7 h in a study area belonging to the Appalachian region. The pulse events of intensity equal or lower than 0.01 mm/hour are considered as part of a no-event period. The storm separation generated a time series of storm intensity, storm duration, and storm depth. Subsequently, we looked at the mean monthly change of the storm depth, storm intensity, and the storm duration. We had to analyze the behaviour of the change more closely in order to classify the catchments into clusters of homogeneous storm characteristics. From this perspective, using climate indices and a synoptic based approach (i.e., Verdon-Kidd and Kiem, 2009) would not help us to get detailed knowledge of the storm characteristics. Our approach serves the goal of our study (i.e., understanding the controls of the FDC shapes at regional scale).

3.2. Simulation of soil moisture: Calibration of SAC-SMA

Under the MOPEX project, default SAC-SMA parameters (*a priori* parameters) have been estimated for each catchment in the dataset to facilitate model calibration (Koren et al., 2003). After calibration, we used the SAC-SMA model output to estimate daily soil moisture and the flow-component FDC.

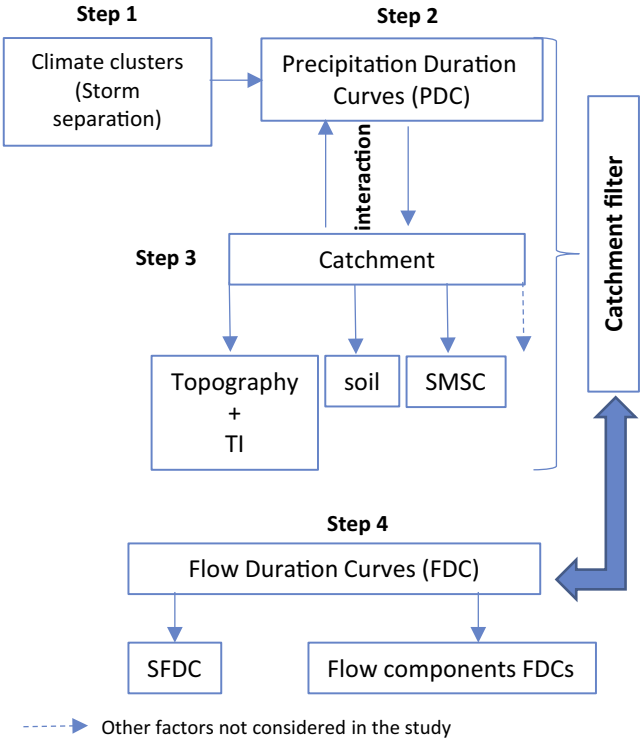

Fig. 3. A conceptual diagram illustrating the workflow of the investigation. In the step 1, we identify the climate clusters. In the step 2, we analyze the precipitation duration curve (PDC) of each catchment in the cluster. In the step 3, we analyze the catchments' properties (topography, soil hydrologic properties, soil moisture storage capacity (SMSC)) except from other factors that deals with the bedrock structure and geomorphology. In the step 4, we investigate the SFDCs (slope of the FDCs) to study the regional variation of the FDCs that results from the interaction between the landscape properties and the precipitation variability (measured by the slope of the PDC). It is the catchment filter stage that assesses how strong the catchment system is in filtering the precipitation. We complement the investigation with analyses of the runoff processes using the topographic index (TI) and the flow component FDCs.

The basic design of the model centers on a two-layer soil structure: a relatively thin upper layer, and usually a much thicker lower layer that supplies moisture to meet the evapotranspiration demands (Koren et al., 2003). Each layer consists of tension and free water storages. The *a priori* SAC-SMA model parameters available in MOPEX were estimated using soil information from a STATSGO soil texture map (Koren et al., 2003). Eleven parameters from a total of thirteen were estimated using soil physical relationships [soil water content (θ_s), field capacity (θ_{fld}), and wilting point (θ_{wlt}) in 11 soil layers] (Koren et al., 2003). The other two parameters do not have a physical meaning—ADIMP and PCTIM deal with the fraction of impervious areas in a catchment. The default ranges by SAC-SMA were initially used for these two parameters. Thus, the model simulations of flows and soil moisture account for the role of the impervious areas. We calibrated the SAC-SMA model parameters using the Shuffle Complex algorithm (SCE-UA) with 10,000 iterations (Sorooshian et al., 1993). This algorithm is extensively used for SAC-SMA calibration to achieve different research goals, such as studying model parameter transferability [e.g. Gan and Burges,(2006)] and building a large database for the continental US (e.g., Newman et al., 2015). Similar to Gan and Burges (2006) and Koren et al. (2003), we constrained the calibration to the *a priori* value of each parameter to keep physical consistency and reduce equifinality. We set ± 35% as the range of deviations allowed from the default parameters. This range is larger than the range used in Koren et al. (2003) (i.e., ±25%). We set this interval to allow for more variability around the default parameters and in the parameters space that is used by the SCE-UA algorithm to find the global optimum. The model was calibrated for the period 1948–1963. The objective function minimized RMSE (Root Mean Square Error) between daily observed and simulated flows. The model calibration performance was evaluated by Nash-Sutcliffe coefficient (NS) (Nash and Sutcliffe, 1970). The catchments with the highest NS were tested for validation and considered in the analyses. Using a sample of 100 catchments for calibration, those with NS lower than 0.50 were disregarded from the study. The eliminated catchments should have a minimal effect on our outcomes (i.e. environmental controls of the FDCs). The same NS based criterion was used by Berghuijs et al. (2014) for analysis of regional water balance in the continental US. In this study, the catchment sample decreased from 100 to 73 and the efficiency of daily simulated flows ranged from 0.50 and 0.92. The average NS value was 0.72. At lower efficiency, mainly peaks of winter (December) and early spring (February) were underestimated. Overall, the model performance was satisfactory. In this study, SAC-SMA simulation helped in predicting the time series of daily flow components and daily soil moisture.

3.3. Soil moisture storage capacity (SMSC)

The soil moisture storage capacity (SMSC) is a surrogate of root zone depth, as described in Gao et al. (2014). It is a reservoir that acts as a dynamic buffer that moderates flows and retains tension water for plant use (Fenicia et al., 2008; Zhao and Liu, 1995). Therefore, SMSC was calculated using daily soil moisture (SM) estimates from the SAC-SMA model. Every year, each catchment has a maximum and minimum value of SM. The difference between the two figures is equivalent to the reservoir of catchment water storage capacity (Gao et al., 2014). The median storage capacity for each catchment was determined and taken as representative.

3.4. Slope of the empirical FDC

The slope of the FDC (SFDC) is a surrogate of the flow variability in time (Sawicz et al., 2011). It is calculated between the 33rd and 66th flow quantile, since at semi-log scale this represents a relatively linear part of the FDC (Yadav et al., 2007; Zhang et al., 2008). The entire daily record of the 50-year (on average) length was used to construct the empirical FDCs and to calculate their slopes. A high slope value indicates a variable flow regime, while a small value means a more damped flow response (Sawicz et al., 2011).

The SFDC is defined as

$$\mathrm{SFDC} = \frac{\ln(Q33\%) - \ln(Q66\%)}{(0.66 - 0.33)} \quad (1)$$

where SFDC is the slope of the flow duration curve, Q33% is the streamflow value at the 33rd percentile, and Q66% is its value at the 66th percentile.

We normalized the empirical FDCs by the mean annual daily flows as in Yokoo and Sivapalan (2011) and Yaeger et al. (2012) before we calculated the slopes of the curves.

3.5. Precipitation duration curve and catchment filter

The PDC is constructed in the same way as the FDC, but instead of daily flows we used daily precipitation (Smakhtin and Masse, 2000). The entire daily record of 50 years (on average) was used to construct the empirical PDCs and calculate their slopes (SPDC). We normalized the PDCs by their respective mean daily precipitation before we calculated the slopes. Unlike FDC, the slope of the PDC usually dips at a smaller percentile than the total 100% because precipitation may be null for many days in a year (Smakhtin and Masse, 2000). Then, the most linear part of the SPDC

calculation will not be equal to that used for SFDC; instead, it will depend on the precipitation records. The linear portion of PDC across the study catchments ranged between 10% and 30%. According to the conceptual framework of Yokoo and Sivapalan (2011), the precipitation is filtered by the catchment system to generate daily flows of a given variability. Here we assumed that the catchment filter can be assessed using the ratio of SFDC to SPDC. Higher values of this ratio correspond to SFDC values that are closer to SPDC; this also corresponds to weaker catchment filters, leading to high flow variability.

3.6. Topographic index distribution for each catchment

Analyses of the topographic index (TI) are helpful to explore the predominant runoff generation. TI represents the propensity of a point within a catchment to generate saturation excess overland flow (Beven and Kirkby, 1979) due to a topographic control on surface and subsurface flows (Rice and Hornberger, 1998). TI was first defined by Beven and Kirkby (1979) as follows:

$$TI = ln(\frac{a}{tan\beta}) \quad (1)$$

where: TI is the topographic index of a point/pixel within a watershed; α is the specific upslope area per unit contour length; β is the local topographic slope angle acting at the point.

In this study, TI was calculated at the pixel level using a DEM of 30-m resolution and algorithms necessary for the determination of specific upslope area "a" and the local slope angle β (Rousseau et al., 2005; Hentati et al., 2010). The TI calculation uses the properties of the stream network, namely, the flow directions and the flow accumulation which both help to identify the riparian zone (see Hentati et al., 2010). Finer details about the stream network dynamics and the stream connectivity are difficult to get for each watershed. Therefore, the effects of intermittent streams and whether they affect the predominant runoff generation mechanism and the flow response are not considered in our calculations of the topographic index and goes beyond the scope of our study.

The frequency of TI distribution was then determined for each catchment after classification of TI pixel values. The differences in the TI frequency distribution at the catchment scale illustrates the wide differences in topographic properties between study catchments and, consequently, the effect of topography on the flow response. According to Beven and Kirkby (1979) and Beven and Wood (1983), large values of TI in tails of the distribution indicate the likelihood of runoff being generated by saturation excess overland flow, whereas smaller values in the tails hint to predominant subsurface processes in the runoff generation. The flow response depends also on the soil infiltration properties and permeability (Price, 2011; Ameli et al., 2015). Therefore, our analyses of the runoff generation mechanism using TI serve to reveal the predominant mechanism that takes place as a response to topography while we acknowledge the effect of other factors (i.e., permeability) on the flow response. We use the spatial pattern of the soil hydrologic properties as indicative of the soil infiltration rates and permeability (Wood et al., 1984). The combination between the soil hydrologic properties and the TI analyses helped in understanding the effect of the runoff generation mechanisms on the regional flow response and the shapes of FDC.

4. Results

4.1. Effects of landscape properties on filtering the precipitation and inducing regional variation of the FDCs

4.1.1. Climate clusters

The Fig. 4a illustrates the catchments classified into three clusters according to monthly changes of average daily storm intensity, storm duration, and storm depth. The storm intensity had the most

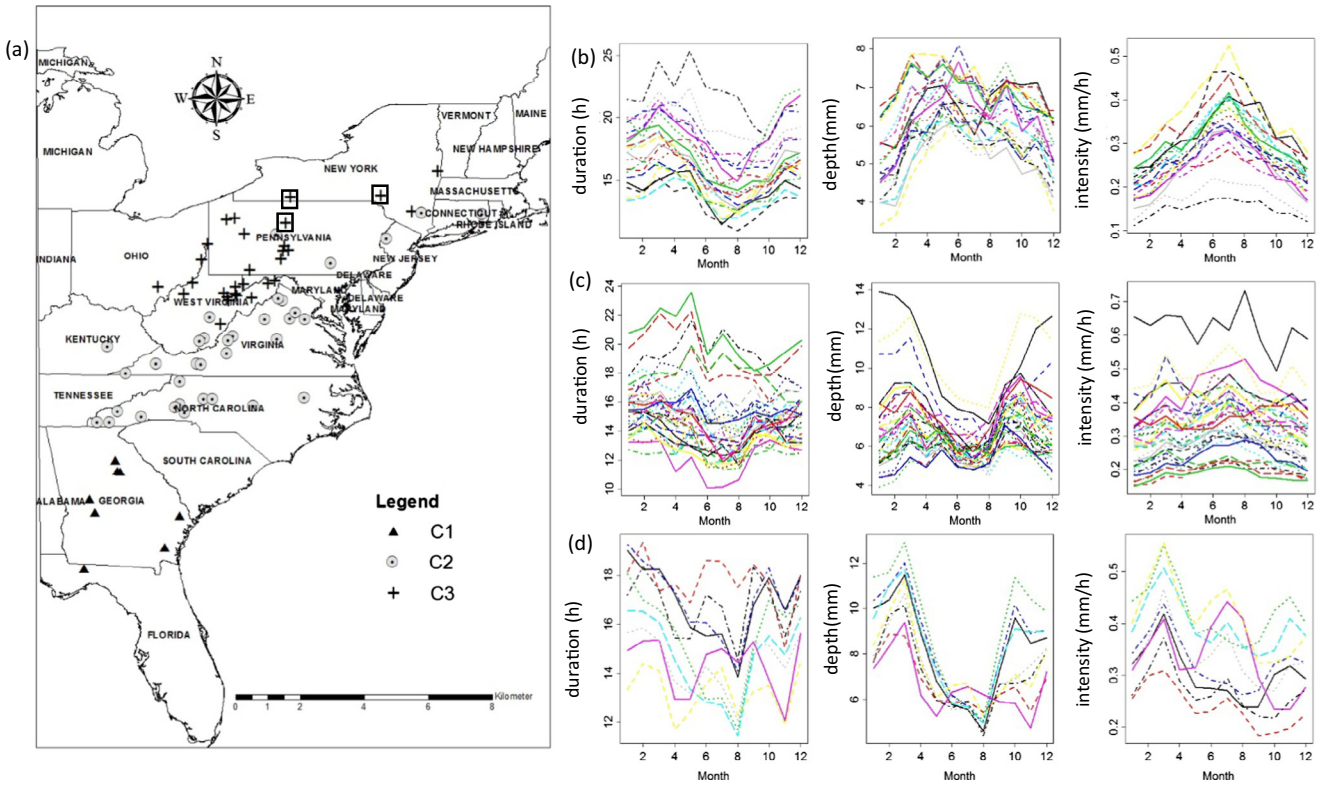

Fig. 4. (a) Catchments classification into three clusters according to storm seasonality (b) seasonal variation of storm characteristics in C3 cluster (c) seasonal variation of storm characteristics in C2 cluster (d) seasonal variation of storm characteristics in C1 cluster. The squares on the map denote the catchments with PDCs dipping at 50%.

systematic regional variation across the eastern US compared to the rest of storm metrics. Therefore, it was the criterion that helped to classify the study catchments into three clusters, or geographically defined regions, of homogeneous storm characteristics. The C3 cluster (Fig. 4(b)) had a peak storm intensity in summer (July). In C2, the storm intensity had no seasonality (Fig. 4(c)). However, in C1 (Fig. 4(d)), we observed two peaks: a first one in summer and a second in late winter. Meanwhile, the storm depth seasonality was similar in C2 and C1 clusters, declining dramatically during the summer and increasing during the fall and winter. In the C3 cluster (northeast), the storm depth was marginally higher in the summer compared to the fall and winter seasons. The duration did not exhibit a seasonal pattern, and its variation is correlated to storm intensity fluctuations. Smaller storm intensities corresponded to larger durations and vice versa. The storms in C3 and C2 clusters had the longest duration (24 h), while in C1 the duration did not go beyond 18 h.

4.1.2. Precipitation variability from slopes of precipitation duration curves

On average, the PDC curves dip at 70% of time exceedance in the C1 and C2 clusters and at 80% for the C3 cluster in the northeastern US (Fig. 5(b), (d), and (c), respectively). These high precipitation percentiles are illustrative of the humid climate in the eastern US. Three catchments in the C3 cluster dip at 50%. They are highlighted by a rectangle in Fig. 4(a). These catchments have a larger number of days with zero precipitation than the rest of the catchments in the same cluster. The MAP for each of these three catchments is in the same range of the average value in the C3 cluster (1100 mm).

The cumulative distribution function (CDFs) of SPDCs in each catchment for each cluster are shown in Fig. 5(a). The clusters of C1 and C2 have the steepest PDCs (high variability of precipitation). In C3, the precipitation is less variable because of flatter PDCs (Fig. 5(a)).

4.1.3. Soil moisture storage capacity

The SMSC (Soil Moisture Storage Capacity) was classified into two groups based on the average of 73 catchments in Fig. 6(a). The figure shows that lowland areas (i.e., in North Carolina, Georgia, and some catchments in Virginia and Pennsylvania) have above average SMSCs compared to highland areas (i.e., high elevations of Appalachian Mountains) where SMSCs are below average. The C1 (Georgia) and C2 clusters are regions where most of the catchments have high SMSC compared to catchments in C3 (Fig. 6(b)). Overall, SMSC increases along North-South and West-East directions. The Forest cover was the lowest in proportions in C2 and C3 (Fig. 6(c)). The SMSCs were the smallest in the C3 because of catchments with highest mean elevations (Fig. 6(d)), and poor drained soils (highest rates of HGC soils, Fig. 6(e).The SMSC was significantly negatively correlated (p-values < 0.05) to forest cover, catchment mean elevation, and HGC soils (Fig. 6(f–h)). Consequently, SMSC is affected by the interaction between forest cover, topography, and soil hydrologic properties. In C2, the SMSC increased as the infiltration rates increased (lower HGC, Fig. 6(e)) and the mean elevation decreased (Fig. 6(a)). In C1, the SMSC was the largest with low mean elevations (Fig. 6(d)), and well-drained soils (lower HGC, Fig. 6(e)). The catchments at high elevation happened to be the most forested (Fig. 6(c)). The SMSC decreased at the most forested catchments (Fig. 6(f)).

4.1.4. The regional variation of the FDC: Categories of flow variability

The FDC slopes were grouped into two categories: SFDCs below and above average. Fig. 7 (a) shows the non-spatial correlation of SFDCs with climate clusters, which demonstrates the dominant effect of catchments' landscape properties in the regional variation of FDCs. The SFDC decreases from northern to southern regions.

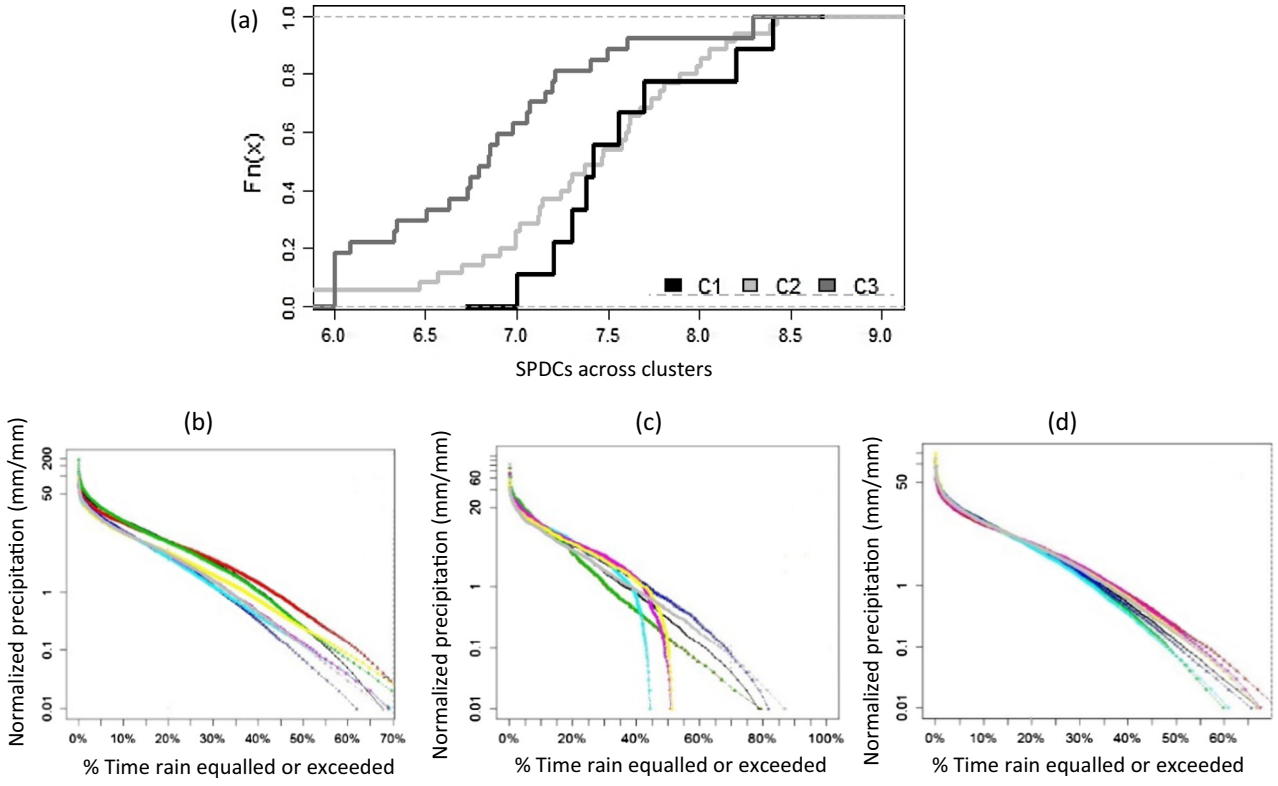

Fig. 5. (a) CDFs of the slopes of PDCs across clusters (b) normalized PDCs in C2 cluster by mean annual daily precipitation (c) normalized PDCs in C3 cluster by mean annual daily precipitation (d) normalized PDCs in C1 cluster by mean annual daily precipitation.

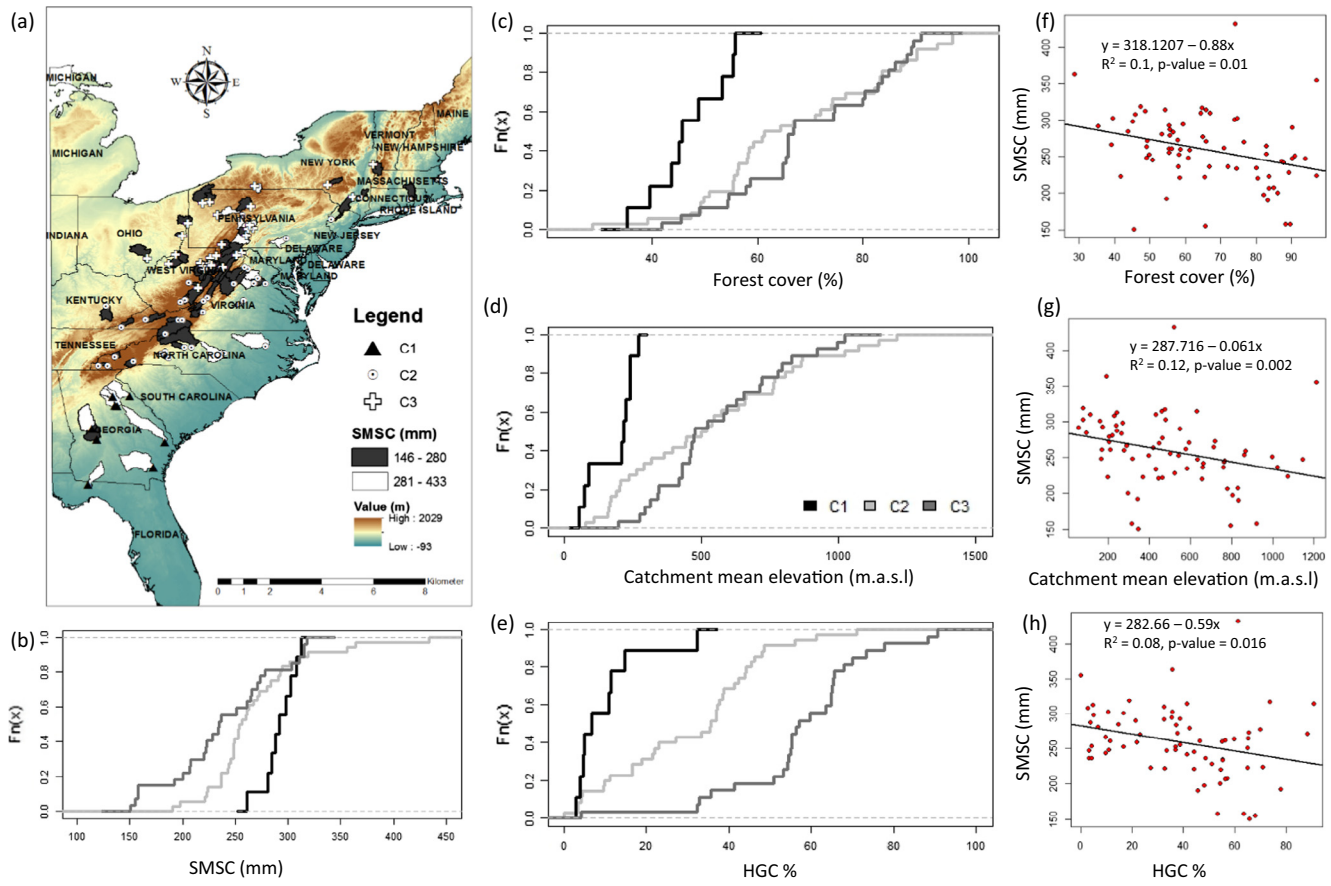

Fig. 6. (a) Regional variation of soil moisture storage capacity (b) cumulative distribution function (CDF) of soil moisture storage capacity (c) CDF of forest cover for each cluster (d) CDF of mean elevation for each cluster (e) CDF of HGC soils for each cluster (f) correlation between forest cover and SMSC (g) correlation between catchment mean elevation and SMSC (h) correlation between HGC and SMSC.

The SFDC is correlated with catchment latitude via a statistically significant relationship ($R^2 = 0.076$, $r = 0.27$, p-value < 0.05). We do not show the figure of the regression for conciseness. The SFDC also decreases in a west-east direction (Fig. 7 (a)) which explains the low R^2 of the SFDC-latitude relationship. Fig. 7 (b), (c), and (d) illustrate the FDC of each catchment classified into clusters of homogeneous storm characteristics. The steepest FDCs (highest SFDC values) are mostly located in the C3 cluster and in some catchments from C1 and C2 (Fig. 7(e)). Most catchments in C1 and C2 had small SFDCs. In Fig. 7(f) and 7(g), the change in the flow variability (SFDC) is related to the change in soil moisture storage capacity (SMSC) and soil hydrologic properties (HGC) (p-value < 0.05). We notice that there is high variability of the SFDC in the 200–300 mm range of the SMSC. The SMSC explains only 4.5% ($R^2 = 0.045$) of the total variability of the SFDC. Thus, in the 200–300 mm range of the SMSC, the FDC may have low or large value of the slopes. This hints at other factors that caused this variability. Also, there is high variability around HGC 0–20% and a small decrease of the SFDC for HGC beyond the 70%. We admit that, in addition to the soil infiltration rates (indicated by proportions of the HGC) and properties of the SMSC, the structure of the subsurface geology and the deep groundwater would have contributed to this variability.

The spatial pattern of SFDC shows that in the northeastern US (C3), most catchments have high flow variability (large SFDCs) and small SMSCs at high elevations where HGC soils are predominant (Fig. 2(b)). The few catchments in C1 (South East) and C2 (Center) with large SFDCS had small SMSCs and soils with medium to slow infiltration rates (half HGC and half HGB). They are mainly located in Kentucky and the interior parts of Virginia (Fig. 7(a)).

Two main particularities in the spatial pattern of the FDCs are worth mentioning. First, there were few catchments in C2 where small SMSC was associated with limited flow variability (small SFDC). These catchments (highlighted by a rectangle in Fig. 7(a)) have predominant HGB soils (Fig. 2). Second, few catchments in North Carolina and South Georgia (highlighted by oval shape in Fig. 7(a)) had large flow variability (high SFDC) in soils with large SMSC and slow infiltration rates (HGC and HGD) (Fig. 3).

4.1.5. Effect of catchment filter on precipitation and flow duration curves

After we analyzed the spatial pattern of the SFDC that changes proportionally to patterns of the landscape properties (mean elevation, HGC, forest cover) and the SMSC, we explore the pattern of the catchment filter. The catchment filter helps to implicitly measure the effect of the catchment system in filtering the precipitation and in generating flow characterized by some level of variability (a value of the SFDC). According to the way it is calculated (ratio of the SFDC by the SPDC), it points collectively to the effect of all the factors that contribute to filter the precipitation (i.e., landscape properties, deep groundwater and the geology structure).

In Fig. 8(a), the filter effect increased from the northern to southern regions. The weakest filters were found in the C3 cluster where the SFDC to SPDC ratio was above average (Fig. 8(a) and (b)). The filters in most catchments from C1 and C2 had below average

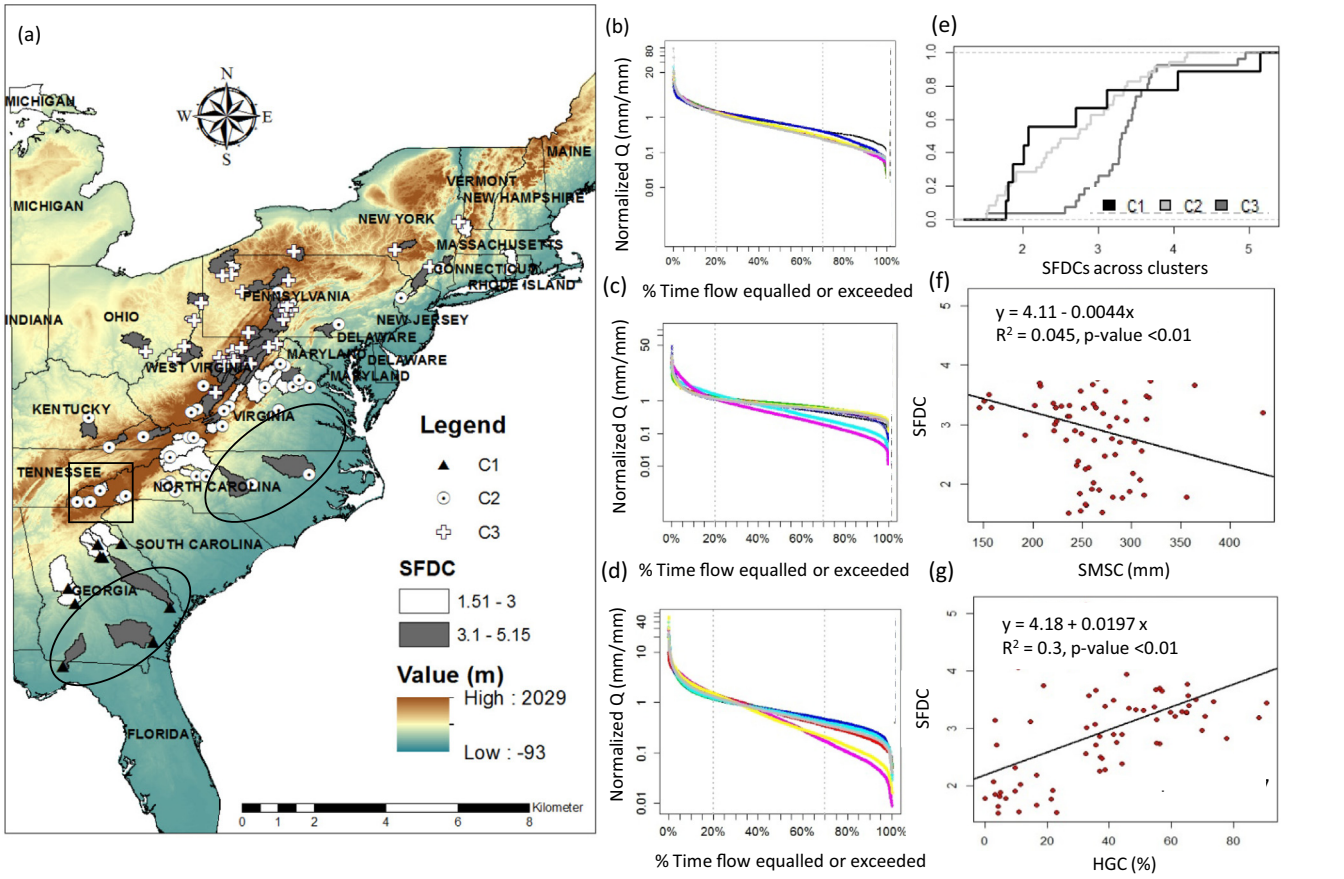

Fig. 7. (a) Regional variation of FDC slopes; the square shape refers to catchments with small SMSC and flat FDC. The oval shape highlights catchments with large SMSC and steep FDC; (b) normalized FDCs in C3 cluster; (c) normalized FDCs in C2 cluster; (d) normalized FDCs in C1 cluster; (e) the CDFs of the SFDCs across clusters; (f) the SFDC-SMSC correlation; (g) SFDC-HGC correlation.

ratios (Fig. 8(b)). The CDFs representing the catchment filters in C1 and C2 illustrate the extent to which they have similar landscape characteristics (Fig. 8(b)). The spatial pattern of the catchment filters in Fig. 8(a) reflects that of FDC in Fig. 7(a). Hence, the FDC shapes are a mirror of the catchment filter effect on the PDC. The characteristics of the catchment filters are related to the soil hydrologic properties and soil moisture storage capacity (Fig. 8(c) and (d)). The effect of the catchment filters on precipitation became more pronounced as HGC rates decreased and SMSC increased (p-value < 0.05).

4.2. Process understanding of the FDC regional variation

4.2.1. Aspect of flow component FDCs

Fig. 9 displays the FDCs of each flow component with regard to SFDC categories (High SFDC versus low SFDC in Fig. 7(a)). The slopes of the baseflow FDCs are of larger values in Fig. 9 (a) for sites with high SFDCs than those in Fig. 9(b) for sites with low SFDCs. We calculated the slope of the median baseflow FDC in each category. It was larger in the category of large SFDCs (slope 3.55) than that of small SFDCs (slope 2.42) (Fig. 9(a), and (b)). This suggests that the total flow variability is partly caused by the baseflow variability. Interflow has a more pronounced contribution to total flow in catchments with large SFDCs compared to those with flat small SFDCs. In fact, it dips between 20% and 70% of the flow percentile for high SFDC category, whereas this happens between 30% and 55% for low SFDC category (Fig. 9(b) and (e), respectively). The normalized median curves confirm these differences (Fig. 10(a) it dips at 47% and at 35% in 10(b)). The surface flow FDCs in the upper tail and until 40% of the distribution are flatter for catchments with small flow variability (small SFDCs in Fig. 9(b)) compared to those with high flow variability (large SFDC catchments category in Fig. 9 (a)). This flow lasts longer and has less irregularities at the lower tail for catchments exhibiting large SFDCs (it dips between 85% and 95% when SFDC is large and between 60% and 80% in when SFDC is small). The normalized surface flow FDCs in both categories were consistent with the differences in the upper tail where surface flow FDC is more regular in the large SFDC category, whereas it showed an inflexion at 40% in the small SFDC category (Fig. 10(a) and (b), respectively).

Consequently, high flow variability stems from a highly variable baseflow, a predominant interflow, and a highly variable surface flow. However, in catchments where the response is dampened (small SFDCs), the baseflow and surface flow are less variable, and interflow contributes less to the total flow variability.

4.2.2. Predominant runoff generation mechanism across the eastern US

From Fig. 11, the TI distributions separated into three distinct groups according to differences in the runoff generation mechanisms across the study catchments (Fig. 11(a)). Three main categories were distinguished: the left skewd, the middle, and the right skewed. In Fig. 11(b), the catchments in the right-skewed TI distribution have large TI values in their tails, which suggests predominant saturation excess overland flow (curve with dashed lines). They spread over the coastal plain and piedmont regions (Fig. 11(a)). However, catchments from the left-skewed TI distribution have smaller values in their tails, which illustrates the preva-

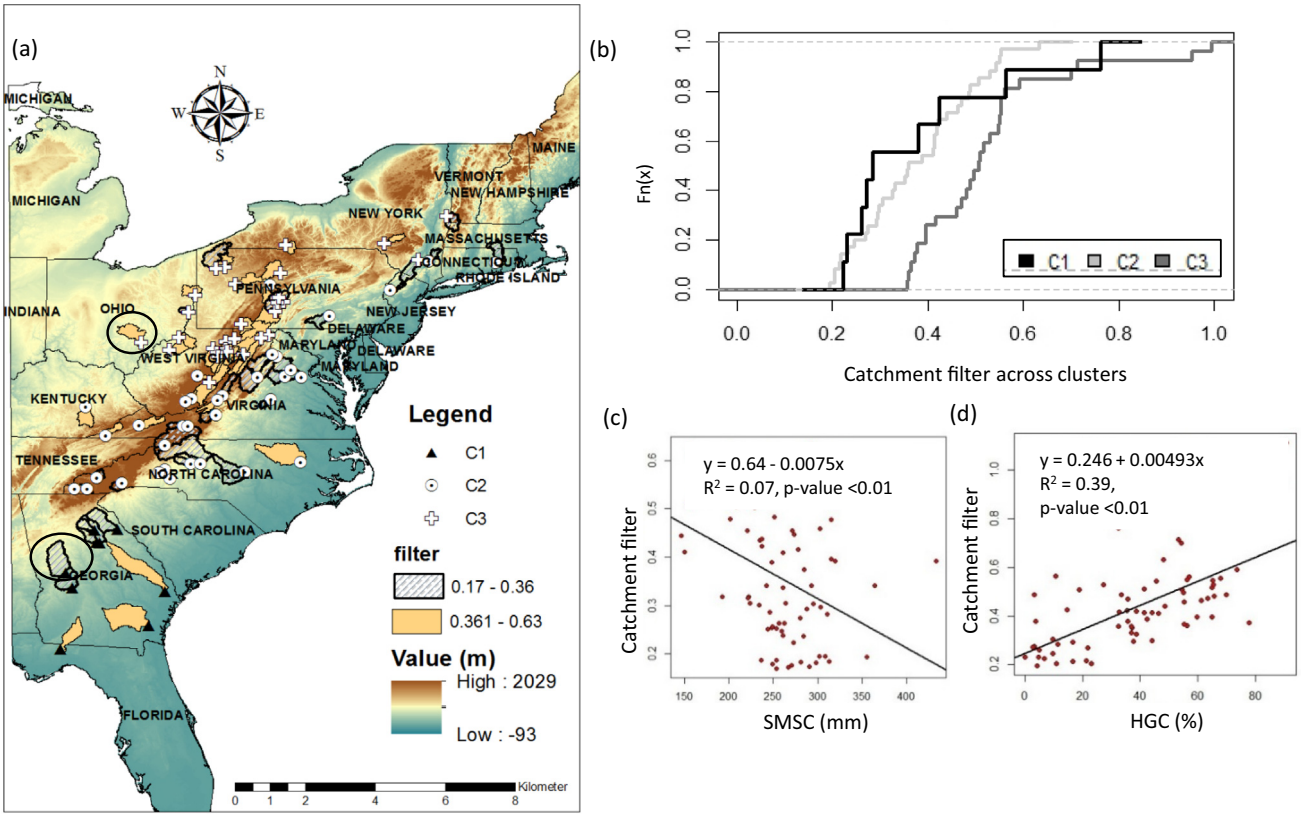

Fig. 8. (a) The spatial pattern of rain filter; the oval shape highlights the catchments we used for the parameter permutation in Section 4.2.3 (b) CDFs of the filter across clusters (c) the correlation between SMSC and the catchment filter (d) the correlation between the proportions of HGC soils and the catchment filter.

lent effect of subsurface stromflow over the saturation excess overland flow (Fig. 11(b)). These are mountainous catchments from the Appalachians (Fig. 11(a)). With regard to the middle TI distribution, it is hard to distinguish a prevalent mechanism. Both mechanisms could be important in their effect on the flow response. The differences of flow component indices and their FDCs across TI categories explained the pattern of the runoff mechanisms. The baseflow indices were consistent (Fig. 12(a) and (d)). However, according to the CDFs of the surface flow index, this latter is higher in catchments with dominant satuartion excess overland flow (right skewed and to some exent the middle TI clusters) (Fig. 12 (d)). The subsurface flow and interflow indices are larger in catchments with predominant subsurface runoff processes (left-skewed TI cluster) (CDFs in Fig. 12(c) and (f), respectively). Fig. 12 compares the FDC flow components using typical catchments in each TI category. The interflow was dominant as a result of prevalent subsurface runoff processes—that is, it dips at 50% and 35% of the distribution in left skewed and middle TI category in Fig. 13(a) and (c), respectively. The interflow effect on the response becomes of lesser importance whenever the saturation excess is dominant (i.e., interflow dips at 30% of the distribution in Fig. 13(b)).

4.2.3. FDC regional variation in relation to the pattern of runoff generation mechanisms

From Fig. 11, the catchments with predominant subsurface processes have large SFDCs (Fig. 7(a) and limited soil moisture storage capacity (SMSC) (Fig. 6(a)). In catchments with large SMSC (Fig. 6 (a)), the prevalent saturation excess overland flow decreases the SFDCs (Fig. 7(a)). It is worth mentioning that in some catchments (highlighted by an oval shape in Fig. 11(a)) with predominant saturation excess and large SMSC (Fig. 6(a)), the SFDCs are of large values (Fig. 7(a)). Also, few catchments with predominant subsurface processes and limited SMSC (highlighted by square shape in Fig. 11(a)) exhibited low flow variability (small SFDCs) (Fig. 7(a)). This seems to conflict with the general pattern of the relationship between FDC shapes and predominant runoff generation mechanism. Other factors interacted with the topography (i.e., soil structure). The soils in catchments highlighted by an oval shape is a combination of HGC and HGB proportions (Fig. 2). Moreover, the soils in catchments highlighted by a square shape are well drained (HGB, in Fig. 2). These combinations are pointing out to the following: whenever saturation excess is predominant, the limited water infiltration could make the flow response less dampened. Also, under predominant subsurface processes, the high infiltration rate mitigates the flow response.

In order to better understand the effect of the infiltration rate on the runoff processes and the FDC shape, we used the parameter permutations between two catchments of different soil properties (HGC versus HGB) and located in the piedmont region (highlighted with ovale shape in Fig. 8(a)). A detailed description of the catchments' main characteristics is provided in Table 1 (Appendix). The saturation excess is predominant in both catchments. The calibrated parameters of the catchment with poor drainage conditions (Fig. 14(a)) are used to simulate flows for the catchment with predominant HGB (Fig. 14(b)). The total flow FDC diverge in catchment number 02349500 from the base conditions (Fig. 14 (c)). The interflow shifted upward, while baseflow diverged from base conditions. The surface flow curve kept the same shape after parameter permutation. Hence, the change in the FDC shapes of interflow and baseflow steepened the total flow FDC.

4.2.4. Flow components of the FDC with regards to precipitation: Process understanding of the catchment filter effect

The effect of the catchment filter on precipitation (precipitation duration curve, PDC) could be demonstrated through the aspect of subsurface and surface processes. From Figs. 13 and 14, the surface

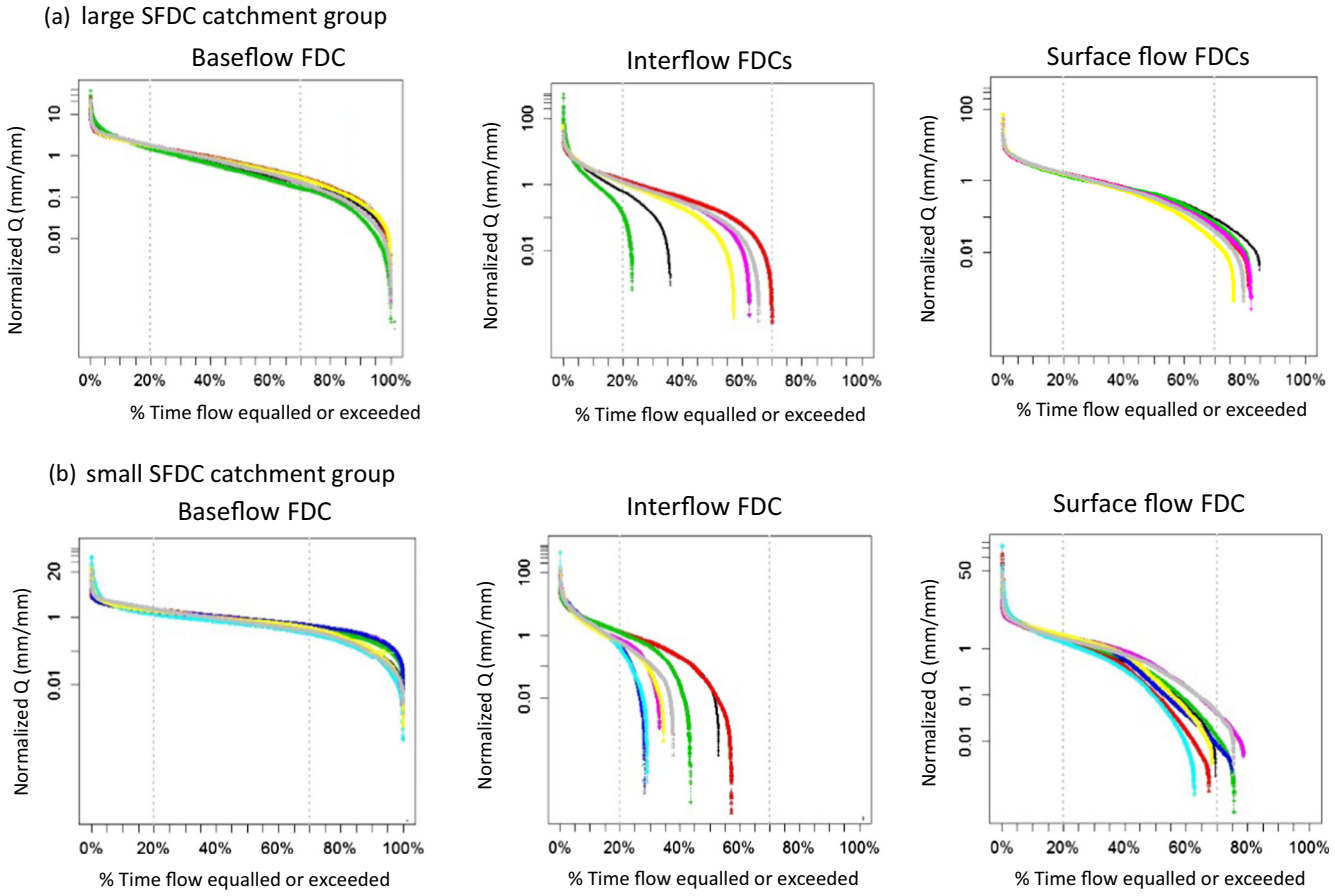

Fig. 9. (a) Baseflow FDC, interflow FDC, and surface flow FDC for catchments with large SFDCs (b) Baseflow FDC, interflow FDC, and surface flow FDC for catchments with small SFDCs. All the curves are normalized by the mean annual daily flow as in Yokoo and Sivapalan (2011).

flow is most sensitive to PDC. The PDC and the surface flow FDC dip at the same percentile contrary to the subsurface flow components (interflow and baseflow). They seem to be less dependent on precipitation and rather more dependent on subsurface processes such as the groundwater and the deep percolation properties of the soils.

Note that the surface flow FDC is almost parallel to the PDC in catchments with predominant subsurface processes and poorly drained soils (Fig. 13(a) and (c)). However, according to Fig. 13(b) and 14(b), the surface flow FDC deviates from the PDC at the upper tail in catchments with small SFDCs under conditions of predominant saturation excess and well-drained soils (HGB). Hence, the catchment filter, although it seems to directly affect subsurface processes, appears to affect surface flow response in catchments with limited flow variability.

5. Discussion

The goal of this paper was to elucidate the spatial pattern of FDCs over the eastern US and to evaluate the interaction between climate and landscape properties with respect to runoff processes in order to provide a comprehensive physical understanding of the regional variation of FDCs. We analyzed rainfall-runoff data from 73 MOPEX catchments. These catchments were classified into clusters of homogeneous storm characteristics in order to control for climate and better inspect the effect of landscape properties.

The storm intensity revealed the most distinct systematic seasonal variation across catchments and was used as a criterion for the classification. The use of other climatic variables (e.g., precipitation and temperature) for climate classification in past studies from the US were less relevant to delineate zones of similar climate (e.g., Fovell and Fovell, 1993). Our cluster delineation using storms was consistent with Hershfield (1961), where in the northeastern US (C3 cluster), the storm intensity has a peak in the summer, in the center it is evenly distributed through seasons (C2 cluster), and in the southeast (state of Georgia in C1 cluster) it shows two peaks during the summer and spring seasons. The climate classification by Coopersmith et al. (2012) in the US split our study area into two clusters based on a combination of climate indices (e.g., aridity, precipitation seasonality, peak of precipitation day) and the average runoff. Most likely, the storm characteristics help to elucidate more details about climate homogeneity, which is critically needed for the study of interaction between climate and landscape properties.

5.1. To what extent the diversity of FDC shapes can be explained by climate and landscape properties?

We found that in the cluster of low precipitation variability (flat PDC) in the northeastern US (C3 cluster) (Fig. 5(a)), the flows had high variability (large SFDCs) (Fig. 7(e)). Also, in clusters of high precipitation variability, (steep PDC) in the central regions (C2 cluster) (Fig. 5(a)), and in southeastern US (C1 cluster in Georgia), the flows had low variability (small SFDCs) (Fig. 7(e)). This finding underlines the effect of the catchments filter when interacting with the precipitation in the process of flow generation. As a result of

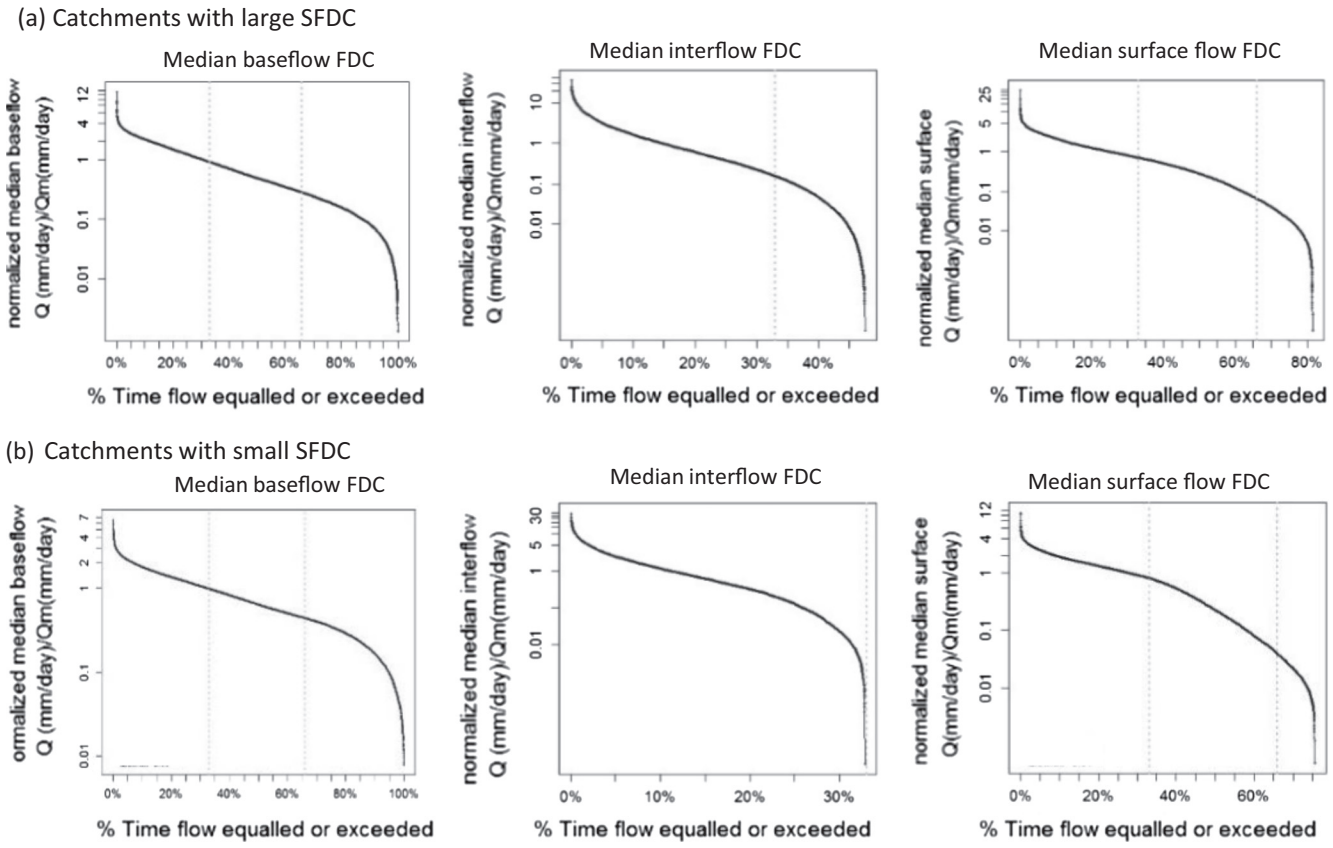

Fig. 10. (a) Median baseflow FDC, median interflow FDC, and median surface flow FDC for catchments with large SFDCs (b) median baseflow FDC, median interflow FDC, and median surface flow FDC for catchments with small SFDCs. All the curves are normalized by the mean annual daily flow (Qm) as in Yokoo and Sivapalan (2011).

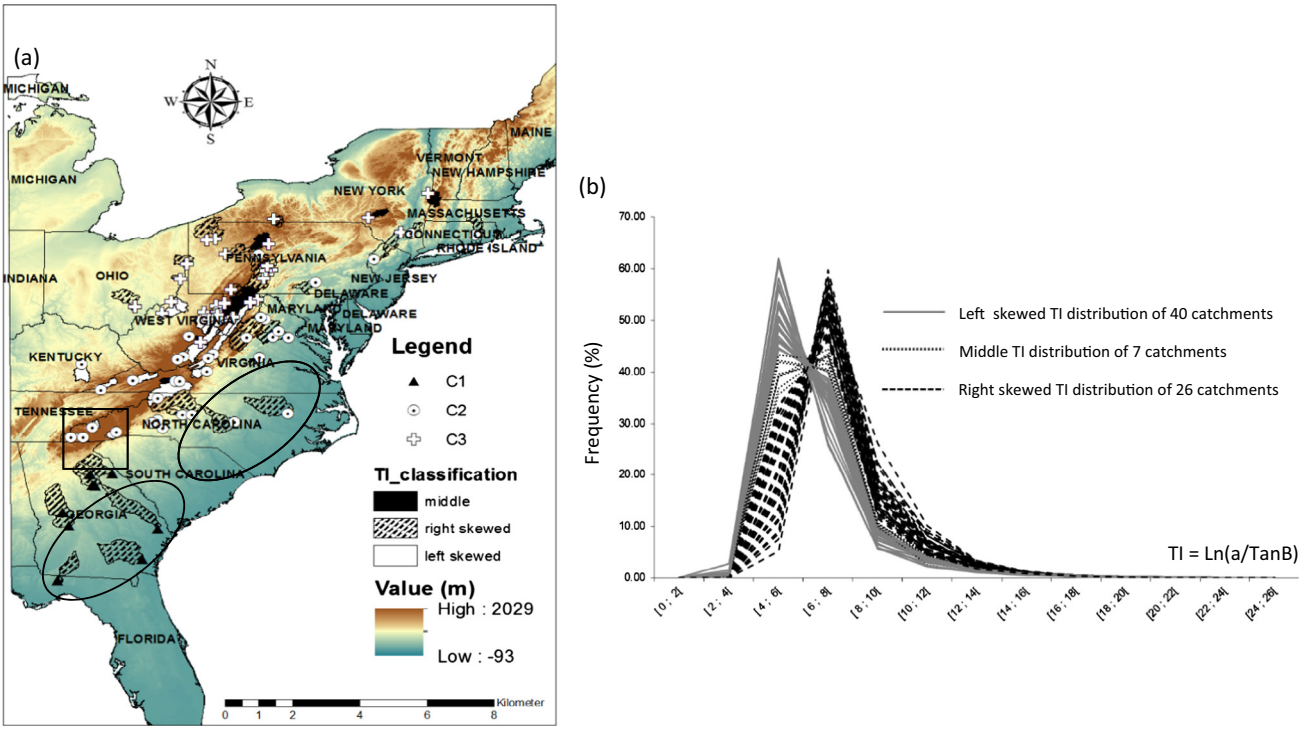

Fig. 11. (a) Spatial distribution of TI groups designated as TI classification in the map; (b) frequency distribution of topographic index per catchment. We identify three groups, the right skewed, the middle, and the left skewed.

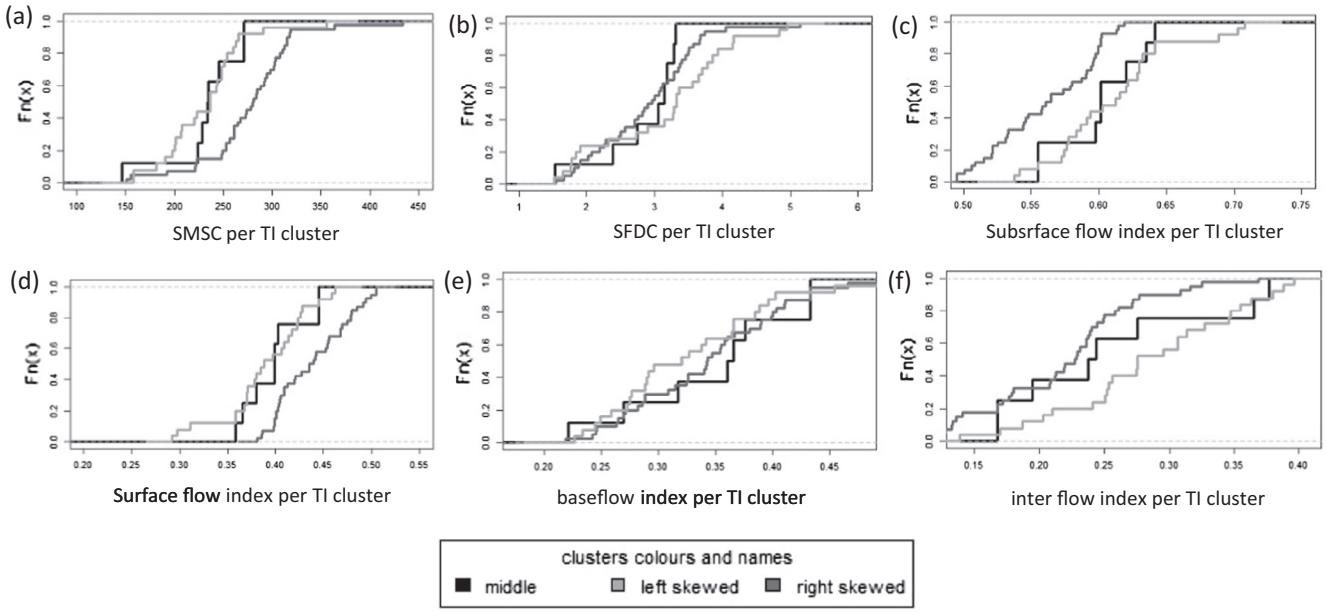

Fig. 12. (a) The CDF of SMSCs in each TI cluster (b) the CDF of SFDCs in each TI cluster (c) the CDF of subsurface flow index per TI cluster (d) CDF of surface flow index per TI cluster (e) CDF of baseflow index per TI cluster (f) CDF of interflow index per TI cluster. The baseflow index was calculated from the ratio of base flow to total streamflow (Schaake et al., 2006). We determined the other flow indices using the same approach. The subsurface flow index was calculated after summing up the baseflow and the interflow.

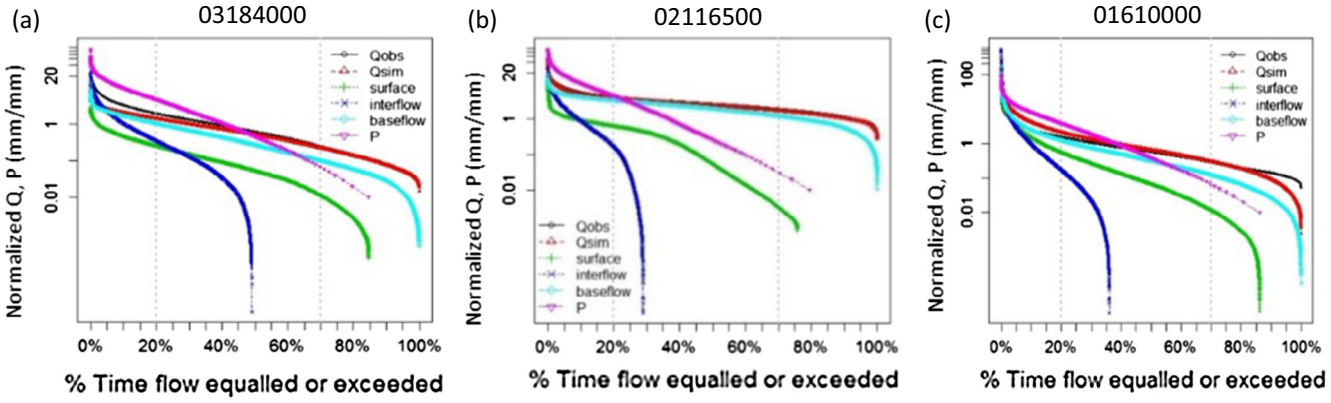

Fig. 13. Flow component FDCs for representative catchments from each TI cluster (a) a catchment from left skewed TI distribution, (b) a catchment from right skewed TI distribution, (c) a catchment from middle TI distribution. *(colour in print).*

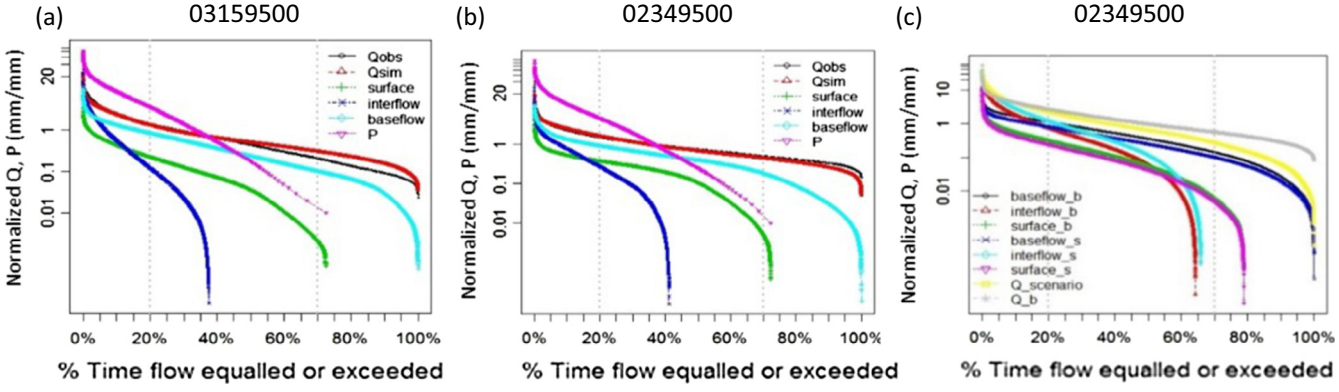

Fig. 14. (a) Flow component FDCs for a catchment with 55% HGC and 30% HGB (b) flow component FDCs for a catchment with 11% HGC and 74% HGB (c) flow components FDC for catchment in (b) using model parameters from catchment in (a). Qobs is observed flow response, Qsim is the simulated flow, P is the daily precipitation. The suffix "b" refers to base conditions prior to parameter permutations. The suffix "s" refers to the permutation scenario. *(colour in print).*

the effect of the catchment filter, the overall pattern was a decrease in the value of slope of FDCs from northern to southern regions and from west to east directions (statistical significant correlation of the SFDC with the latitude, p-value < 0.05)

In this study, mainly we reveal the effect of the interaction between the soil moisture storage capacity (SMSC), the soil drainage conditions, and the topography in characterizing the catchment filter (Figs. 6 and 8) whose spatial pattern (Fig. 8(a)) mirrored the regional variation of the FDC (Fig. 7(a)). In past FDC regionalization studies, some of these landscape properties (mean elevation, soil types, and land cover) have been used as explanatory variables to regionalize FDC without being explicitly analyzed in terms of their effect on the flow variability. For example, Arora et al. (2005) used the mean elevation to distinguish between regions of different FDCs. Sefton and Howarth (1998) deployed a combination of landscape characteristics (e.g., topography, soil types, climate, and land cover) for FDC regionalization.

Most of the large (small) SFDCs are located at high (low) elevation (Fig. 7(a)). However, there are few catchments, in C1 and C2 clusters, despite they are at high (low) elevation they have small (large) SFDCs (highlighted by square and an oval shape in Fig. 7(a), respectively). In the following, we discuss first the reasons for large (small) SFDCs at high (low) elevation. We found that most of the catchments in C1 and C2 acted as a strong precipitation filter (Fig. 8(b)) due to large SMSC (Figs. 6(b) and 8(c)) and large soil infiltration rates (Figs. 6(e) and 8(d)). Whereas the catchment filter in C3 was weaker (Fig. 8(b)) because of small SMSC at high elevation (Figs. 6(b) and 8(c)) and poorly drained soils (Figs. 6(e) and 8(d)). A study by Swift et al. (1988) demonstrated that the decreasing soil depth in steep topography resulted in less opportunity to store soil moisture before a rain. Also, Swift et al. (1988) study suggested that, at higher elevation, there is a limited evapotranspiration demand. In our study region, we found that the potential evapotranspiration (PET) decreased with elevation, which supports the idea of decreased ET at high elevation and its effect on enhancing the flow variability. The figure of the PET spatial pattern was not shown for conciseness. In conditions of catchments at high elevation, Butt et al. (2001) stated that the steep topography indicates the hydraulic gradient of shallow soils. These physical explanations that combine the decrease of the soil moisture storage capacity with the decrease of ET and the increase of the hydraulic gradient—under conditions of steep topography—corroborate our findings and help to understand the controls of large values of the SFDCs at high elevations (in catchments of the C3 cluster and a few in C1 and C2 clusters). Our results, also underscored the effect of the soil properties on shapes of the FDCs (the increase in the HGC proportions steepened the slope of the FDCs (Fig. 7(g)). According to Price (2011), the influence of soil characteristics on water storage can be understood by the tight correlations between soil properties and topography. The soil properties play a significant role in the rate of soil moisture loss due to surface or subsurface topographic gradients (Dodd and Lauenroth, 1997; Yeakley et al., 1998). Therefore, large values of slope of the FDCs at high elevations in C3, and in a few catchments from C1 and C2, could be related to the interaction of shallow soils with poor drainage conditions. This effect is maximized in C3 where the SFDCs were the largest (Fig. 7(e)) and close to the precipitation variability (slope of PDC) (Fig. 8(a)). In contrast to conditions of large SFDCs, the mitigated flow response (small SFDCs) in most catchments from C1 and C2 could be explained by the interaction of flat topography with soils of high infiltration rates (HGB). The increased water storage capacity (large SMSC) dampened the flow variability despite the large precipitation variability.

We should mention that, in our study, the effect of the vegetation cover on the flow variability was, overall, not as explicit as the effect of topography and soil drainage conditions. In fact, the contrast in types of the vegetation cover between the study catchments is not as pronounced as it is for topography and soil hydrologic properties. The vegetation cover is consistent and decreases in few catchments in piedmonts and the southeastern US (see Fig. 8 in Berghuijs et al. (2014)). Therefore, the vegetation cover effect was rather implicit to that of soil moisture storage capacity (statistically significant correlation between SMSC and forest cover proportions in Fig. 6(f)).

With regard to conditions of large SFDCs at low elevations (in southern Georgia (in C1) and in the east coast (in C2)) and small SFDCs at high elevations (in C2) (Fig. 7(a)), this finding could explain the considerable scatter we found for the SFDC-SMSC correlation (p-value < 0.05) (Fig. 7(f)) compared to the SFDC-HGC relationship (p-value < 0.05) (Fig. 7(e)). The decrease in SMSC, due to elevation, while it is associated with large SFDCs should not be taken as a general pattern. There are other factors, apart from the elevation, that control the FDC shapes. We conjecture the effect of the groundwater (implicitly considered in soil moisture simulations of the SAC-SMA model) and the geology structure that are not investigated because of limited data availability. Nonetheless, the landscape properties (i.e., soil hydrologic properties, forest cover) interacting with the SMSC pattern help in framing an explanation. The SMSC correlates with the forest cover, mean elevation, and soil hydrologic properties (Fig. 6(f)–(h)).

At high elevations (small SMSC) in conditions of small SFDCs, the large infiltration rate allows for the rain water to move downward to the root zone. In presence of forest cover, the water might have been used by the forest (i.e., transpiration and interception) to allow for additional storage as ET takes place (Bonell, 1993). Hence, less water is stored in the soil leading to dry antecedent moisture conditions prior to the rain event. It has been shown repeatedly, particularly by isotope hydrology, that pre-event conditions, mainly the antecedent moisture conditions, affect the flow response (McDonnell 1990; Sklash and Farvolen, 1979). In a study by Burt and Swank (1992) the forest cover explicitly reduced the flow response by affecting flow magnitudes and their respective frequency. The FDCs were of lower value of the slope compared to those from other vegetation types. The dry antecedent moisture conditions due to the effect of the forest cover mitigates the flow for all ranges of the precipitation events (small and extremes). This effect remains true for small to medium flows based on deterministic chronological pairing approach (Bathurst, 2014) as well as for extreme flows based on stochastic frequency pairing approach (Birkinshaw et al., 2011, Fig. 8; Crooks and Davies, 2001, Fig. 6; Reynard et al., 2001, Fig. 5) Therefore, it appears that, in the few fully forested catchments at high elevations, the small SFDCs are related to the effect of the interaction between the forest cover and the large infiltration rate on the antecedent moisture conditions and consequently on the flows' magnitude and frequency. With regard to the condition of large SFDCs at low elevations, most likely the low infiltration rates (dominant HGC soils) did not allow to damp the flow response despite the large SMSC. One should not forget the effect of below surface geology and its role to advance the understanding of the flow variability controls, particularly in mountainous areas (i.e., Di Matteo et al., 2017; Kelson and Wells, 1989). This dimension is again not covered in the present research because of lack of data.

Our results from the empirical analysis partially agree with the hypothesis of Yokoo and Sivapalan (2011) that stems from a theoretical numerical study, where it has been suggested that slope of the FDCs in shallow soils are steeper than those in deep soils. It is

true that most catchments in the present study region have large (small) SFDCs at high elevations in conditions of small (large) SMSC. However, the exceptions we found make the generalization hampered by the soil hydrologic properties, in addition to other factors related to the subsurface geology.

One may suggest that when SMSC is large and the soil is poorly drained, the flow variability could be high (close to precipitation variability) because of limited infiltration rates. The FDCs can be of low values of the slope despite of the small SMSC if the soil is well drained. The effect of landscape properties on steepening the FDCs is maximized (in C3 cluster) if the poor drainage conditions and small SMSCs on steep topography are combined. The several hypotheses that emerge from our empirical analyses require further testing using several degrees of landscape complexity when interacting with the climate.

5.2. Process-based understanding of the spatial pattern of FDCs

The process-based analyses of the spatial pattern of SFDCs revealed that catchments with large SFDCs mainly (in C3 cluster and in few catchments from C1 and C2) have a larger proportion of interflow and steep slope of the surface flow FDCs (Figs. 9(a), 10(a)) than catchments with small SFDCs. The runoff flow components have different velocities: usually, surface flow is the fastest response followed by interflow and baseflow. Previous studies found that subsurface flow (sum of interflow and baseflow) can be as fast as surface flow (e.g., Sklash and Farvolen, (1979). These properties imply that high flow variability (large SFDCs) can be related to the predominance of fast-flow components on the response. Also, we found that more variable total flow corresponds with steeper slope of the baseflow FDCs (as well as larger slopes of median baseflow FDCs; see Fig. 10). This result suggests that baseflow characteristics vary with catchment conditions and, although it is a slow response, it also affects the overall flow variability. This hints at the effect of groundwater associated with the geology of soils below surface (i.e., Di Matteo et al., 2017).

The TI analyses showed that most catchments with large SFDCs had left-skewed TI distributions with small values in their tails. This fact leads to predominant subsurface flow processes in the runoff generation routine (Beven and Kirkby, 1979) illustrated by large interflow index hinting at limited groundwater effect. The predominant landscape properties in catchments with large SFDCs (limited SMSC, steep topography, and poor drainage conditions) and the properties of the surface and interflow responses indicate that the FDC shape illustrates the effect of limited runoff contributing area (small TIs in tails). Likely, the hydraulic gradient is the major regulator of the response (Hewlett and Hibbert, 1967).

Another significant aspect deals with the effect of soil infiltration rates in the runoff processes (a combination of HGB and HGC or fully HGC). In catchments of large SFDCs, the surface-flow FDCs were of more regular shape than in catchments of small SFDCs (all dip at 80% in Fig. 9(c) versus 60 to 80% in Fig. 9(f)). The small infiltration rates in catchments with large SFDCs—mostly located in hillslopes—suggest that the infiltration excess overland flow is dominant in the process of surface flow generation (Beven and Wood, 1983). Guebert and Gardner (2001) found that on steep slope catchments the surface flow response becomes faster when it is dominated by the infiltration excess mechanism. Therefore, the large SFDCs illustrate the culminated effect of the infiltration excess surface flow and the interflow. The effect of this combination could be of major impact in C3 catchments due to larger proportions of HGC soils compared to the rest of catchments in C1 and C2 of the same large SFDC category.

With respect to the small SFDCs, that represent most catchments in C1 and C2, the proportion of interflow from the total flow is low (Fig. 10(b)). The surface flow FDCs at the upper tail as well as the median slope of the baseflow FDCs are flat (see Fig. 10(b)). In these catchments, the increase of TIs in the tails make the TI distributions right-skewed (Fig. 11(b).) TI increases as contributing area increases and slope angle decreases (see Eq. (1)), hinting to a well-developed riparian zone (Beven and Wood, 1983). Usually, the more developed this zone the deeper the soils, allowing for more infiltration until saturation. The runoff response under these conditions is dominated by saturation excess overland flow. The excess water runs as surface runoff due to saturation excess overland flow (Beven and Wood, 1983). The aspect of runoff processes in most catchments from C1 and C2 and the landscape properties (large SMSCs and high proportions of HGB soils), suggest that the saturation excess dampens the flow response as a result of flat topography and large infiltration rates. Likely, the increase of groundwater levels, in catchments with small SFDCs at low elevations, slows down the surface flow, limits the interflow contribution and enhances the baseflow.

As pointed out in the previous Section 5.1, the FDCs could be flat in conditions of small SMSC and well-drained soils. The TI analyses classified these catchments (highlighted by square shape in Fig. 11(a)) under a predominant subsurface runoff processes category. Likewise, other catchments with prevalent saturation excess have small SFDCs in presence of poorly drained soils (highlighted by oval shape in Fig. 11(a)). Both findings support the idea about the influence of infiltration rate in affecting the runoff processes. In the literature, the infiltration rate is associated with soil depth, topography, and hydrologic characteristics (Weiler and McDonnell, 2007), and it is a chief regulator of the flow response (Guebert and Gardner, 2001). Therefore, in the catchments with small values of the SMSC and the SFDC, the impact of the predominant subsurface stormflow at hillslopes could have been lessened by the high infiltration rates that reduced the interflow contribution (Fig. 12(f), respectively). Under similar conditions, Guebert and Gardner (2001) stated that on catchments at high elevation, the landscape features in combination with high infiltration rate may produce a significant overland flow by saturation excess mechanism. The saturation in hillslope catchments is controlled by both the topography and the permeability of soil layers (Graham et al., 2010). More research is required to elucidate the relative role of saturation excess on the flow response when subsurface stormflow is dominant in hillslope catchments of well-drained soils.

The results from parameter permutations between catchments at low elevations and of opposite soil hydrologic properties (HGB versus HGC) explained the case of large SFDCs at low elevations. The lower infiltration rate steepened the total flow FDC because the interflow shifted upward, and the baseflow diverged from base conditions (Fig. 14(c)). This outcome is consistent with Beven and Germann (1982), who stated that fine soil texture limits groundwater influence. Also, Bonell (1993) reported that in forest environments, the infiltration excess overland flow may occur in combination with saturation excess overland flow owing to properties of lower infiltration. Therefore, a predominant saturation excess may lead to a less dampened response because of limited drainage conditions. This is probably the most plausible physical explanation for the shapes of FDCs in the few catchments we question here.

With regard to the effect of the PDCs on the flow component FDCs as a response to the interaction with the catchment filter, the subsurface flow FDCs were not sensitive to the precipitation

behaviour but were rather directly affected by the catchment conditions. Only surface flow FDC tracked the PDC, as suggested by Yokoo and Sivapalan (2011). However, in typical catchments with small SFDCs, the surface flow FDC and PDC were not parallel, as in the theoretical study of Yokoo and Sivapalan (2011), but rather diverged at the upper tail (> 40% of the surface flow percentile) (Figs. 13(b) and 14(b)). Therefore, for conditions of dampened flow, catchment characteristics have a major role in filtering the precipitation even at the level of a fast response.

6. Conclusions

The state of knowledge about FDCs lacked physical understanding about the controls underpinning their regional variation. Our study helped to advance our physical understanding by investigating the interaction of climate and landscape properties and the innate runoff processes responsible for the disparities in the shapes of FDCs. Using 73 catchments from the eastern US, we highlighted strong regional differences within and across clusters of homogeneous storm characteristics.

The FDC shapes were attributed to the filter effect of landscape properties on precipitation. This effect was pronounced so that regions with high precipitation variability had limited flow variability (small SFDC). On the other hand, the regions with low precipitation variability had the highest flow variability (large SFDC). The flow response was dampened (small SFDC) in catchments at low elevations of well-drained soils and large storage capacity. These characteristics led to predominant saturation excess overland flow that allowed for more infiltration to lower layers, enhanced baseflow, and limited interflow. The largest slope of the FDCs were associated with steep topography, soils of small storage capacity, and low infiltration rates. This interaction led to dominant subsurface stormflow and surface flow generated by infiltration excess overland flow.

This paper also demonstrated that the effect of soil infiltration rate on FDC shapes was pronounced such that small (large) SFDCs at low (high) elevations is not always a general pattern. At low elevation and large soil moisture storage capacity, the catchments with predominant saturation excess experienced high flow variability (large SFDCs) because of poor drainage conditions. Also, in shallow, well-drained soils at high elevations, the prevalent subsurface stormflow led to limited flow variability and small SFDCs.

For all of the process-based analyses, the surface flow was the flow component most directly affected by the precipitation variability. However, this relationship became less important in catchments with small SFDCs. This result suggests that both the subsurface flow components (interflow and baseflow) and the surface flow, are highly affected by the dominant filter effect dictated by the landscape properties.

The limited availability of detailed descriptors of geology, geomorphology, and the groundwater levels (covering a large region) points out that we are also limited with respect to understanding subsurface controls (see as example Di Matteo et al., 2017). More limitations deal with the need to investigate in more detail the impact of the stream hydrological properties and the vegetation type (i.e., species, age, density) on the FDC shapes. Our results need to be complemented by an investigation of the effect of the catchments geomorphology and the vegetation type.

With regard to whether our analysis of the FDC controls have considered the non-stationarity in streamflow response caused by either land use or climate variability (i.e., Milly et al., 2008), our study catchments have limited anthropogenic activities. Therefore, non-stationarity in streamflow is due mainly to natural fluctuation caused by ENSO (El Niño Southern Oscillation) (Sivapalan and Samuel, 2009). The fifty years of observed flow data would be subject to cyclical fluctuations of wet and dry years. Consequently, our physical understanding of the FDC controls could potentially change depending on whether we investigated only flow records representative of dry or wet years. One of the potential changes would deal with more visible differences in the shapes of the FDC that illustrates more explicitly the effect of groundwater levels. We recommend to address the effect of ENSO on understanding the FDC controls in future studies. Also, one should mention—in addition to the ENSO effect—that the FDC controls we quantify in this study may not hold in the future under non-stationarity caused by future anthropogenic climate or land use change.

Despite the limitations, the physical understanding we gained is key for future works related to process-based FDC predictions. This research venue will further advance the understanding and can be used to solve issues of predictions in ungauged basins. Following our empirical approach, more research is needed to study the regional change of flow variability in other regions within the US and elsewhere around the world to either corroborate or refute our hypothesized conclusions and address the limitations of our analysis. We believe that our empirical study can be aided by numerical experiments such as Yokoo and Sivapalan (2011) to test our hypotheses and investigate the climate interactions with complex physical features affecting the flow variability.

Acknowledgements

We thank the three anonymous reviewers for their careful reading of our manuscript and their many insightful comments and suggestions. A special thanks to W. Berghuijs for providing part of the data used in the study. We are grateful to Pr. Murugesu Sivapalan from the University of Illinois at Urbana-Champaign for valuable guidance during early stages of this work and for fruitful discussions on the findings and the earlier draft of the manuscript.

Funding

W. Chouaib is grateful for the Islamic Development Bank (IDB) who funded her PhD studies at the University of British Columbia. This study was partially funded by internal awards of the Faculty of Forestry: [Weldwood of Canada Limited H. Richard Whittall, 2016], [Mary and David Macaree, 2015], and [Peter Rennie Memorial Award, 2017]) and the NSERC – Canada Discovery Grant of Dr. Younes Alila (RGPIN 194388-11).

Authors' contribution

W. Chouaib analyzed the data and wrote the manuscript. Y. Alila supervised both the content and interpretations of this work and edited the manuscript. P.V Caldwell helped with fruitful discussions on the findings and edited the manuscript.

Appendix Table 1. The catchments' descriptors of the study region.

ID	Long	Lat	HGA	HGB	HGC	MEAN ELEV	SLOPE	URB	FST	AGR	OPEN WATER	WET LAND	MAP	PET	SDR	AI	RR	PSI	Area (km^2)
01031500	−69.315	45.175	4.5	14.3	41.4	299.4	6.5	2.2	77.4	1.8	2.13	5.67	1180.0	512.5	39.3	0.43	0.54	0.03	769.05
01057000	−70.540	44.304	15.3	13.6	59.2	281.8	11.7	4.2	83.9	3.6	1.57	3.61	1083.3	559.3	36.2	0.52	0.51	0.03	190.92
01127000	−71.985	41.598	11.0	34.5	37.1	164.4	5.1	11.4	60.9	10.1	2.69	12.97	1273.3	624.1	27.8	0.49	0.47	0.03	1846.70
01170100	−72.671	42.703	2.4	25.4	54.2	410.9	13.6	3.0	90.8	4.4	0.38	1.28	1307.8	563.3	34.3	0.43	0.56	0.02	106.99
01334500	−73.378	42.939	5.8	21.6	55.4	430.1	15.4	7.2	74.4	13.6	0.33	2.12	1198.9	573.8	30.3	0.48	0.43	0.09	1320.90
01371500	−74.166	41.686	8.3	6.9	64.9	196.1	6.1	11.6	41.8	30.5	1.27	13.45	1186.2	652.2	22.6	0.55	0.45	0.06	1841.48
01372500	−73.873	41.653	8.6	38.9	46.4	166.4	7.1	9.0	56.1	24.2	0.70	4.37	1148.4	645.7	24.4	0.56	0.46	0.07	468.80
01411300	−74.821	39.307	12.0	45.7	14.7	16.2	0.3	1.2	73.8	9.8	0.01	13.31	1125.0	751.7	13.3	0.67	0.37	0.02	79.37
01413500	−74.653	42.145	0.0	0.0	74.1	769.1	19.8	0.6	98.2	0.3	0.09	0.60	1520.2	502.5	34.1	0.33	0.51	0.08	434.00
01423000	−77.957	42.122	4.4	2.2	88.3	591.6	15.7	3.9	65.8	27.5	0.24	1.12	1120.1	554.8	28.7	0.50	0.44	0.09	859.90
01445500	−74.979	40.831	6.9	32.0	37.7	204.0	6.4	9.9	49.1	26.2	1.42	11.64	1245.8	646.8	22.7	0.52	0.45	0.07	274.50
01541500	−78.406	40.972	6.8	24.2	61.2	520.5	9.5	7.1	74.2	15.8	0.98	0.00	1062.0	593.0	24.0	0.56	0.46	0.11	960.90
01543500	−78.103	41.317	0.5	47.9	51.0	521.9	18.3	1.5	89.2	2.7	0.08	0.60	1096.0	593.1	25.4	0.54	0.46	0.10	1774.20
01547700	−75.140	42.166	6.8	32.3	50.0	395.7	17.8	4.7	84.4	10.9	0.01	0.00	1048.5	635.4	21.9	0.61	0.43	0.10	113.54
01552000	−78.103	41.317	1.6	3.3	88.0	509.3	13.0	2.6	81.6	10.7	0.37	0.18	1134.1	580.8	26.5	0.51	0.49	0.08	1129.49
01552500	−77.606	41.060	0.0	0.9	91.1	562.6	15.7	2.6	75.5	8.6	0.17	0.00	1228.5	561.5	27.9	0.46	0.55	0.07	60.64
01574000	−76.720	40.082	2.9	51.4	35.6	189.7	4.8	9.3	28.6	59.0	0.59	0.95	1086.1	720.6	17.2	0.66	0.35	0.05	1320.90
01608500	−78.654	39.447	14.4	21.4	54.6	655.8	20.9	3.9	80.4	15.2	0.48	0.00	1003.3	642.9	17.4	0.64	0.47	0.09	3809.90
01610000	−78.458	39.537	16.1	18.1	55.4	583.0	17.8	4.8	80.0	13.9	0.66	0.06	1022.7	647.9	18.2	0.63	0.46	0.08	8052.30
01628500	−78.755	38.322	0.4	55.4	37.0	540.5	11.3	11.6	49.8	38.2	0.32	0.00	1056.1	678.7	14.5	0.64	0.39	0.08	2807.60
01631000	−78.211	38.914	0.4	53.0	38.6	500.9	12.7	10.5	55.4	33.5	0.59	0.01	1070.9	685.9	14.4	0.64	0.38	0.07	4252.80
01634000	−78.336	38.977	0.7	42.4	44.0	442.6	12.8	6.8	58.4	34.4	0.43	0.00	982.1	697.6	13.6	0.71	0.37	0.09	1989.10
01664000	−77.814	38.531	0.0	59.0	35.5	237.2	10.0	4.1	59.3	35.9	0.26	0.19	1135.9	730.4	11.8	0.64	0.35	0.08	1605.80
01667500	−77.975	38.350	0.0	56.3	37.2	263.4	10.4	6.2	56.4	36.5	0.40	0.26	1185.5	741.6	10.6	0.63	0.36	0.07	1222.50
01668000	−77.518	38.322	0.0	44.5	42.5	202.3	8.0	4.5	55.6	38.1	0.42	0.30	1145.1	748.6	10.9	0.65	0.36	0.07	4133.60
02016000	−79.760	37.792	1.0	40.9	41.3	661.1	18.0	3.6	87.7	8.3	0.39	0.00	1063.9	667.7	16.0	0.63	0.44	0.05	1194.00
02018000	−79.912	37.666	0.4	53.3	33.4	635.0	18.1	3.1	90.1	6.4	0.34	0.00	1089.2	668.2	11.3	0.61	0.39	0.07	852.10
02030500	−78.378	37.703	0.0	71.1	16.6	157.1	3.8	2.8	73.9	12.3	0.22	1.40	1145.4	775.4	8.5	0.68	0.37	0.04	585.30
02055000	−79.939	37.258	0.9	35.7	56.1	575.1	17.2	18.7	70.8	10.3	0.09	0.01	1058.5	687.4	10.8	0.65	0.36	0.07	1023.10
02083500	−77.533	35.894	10.1	55.3	19.0	76.7	2.0	7.5	47.4	27.5	0.65	7.80	1181.9	835.9	4.3	0.71	0.35	0.05	5654.00
02102000	−79.116	35.627	1.3	55.7	38.7	171.0	3.3	11.7	55.4	22.7	0.58	0.85	1203.3	839.9	4.2	0.70	0.37	0.04	3714.10
02116500	−80.386	35.857	1.0	78.9	16.6	395.2	9.5	12.8	58.1	23.1	0.43	0.21	1238.8	773.2	7.7	0.62	0.47	0.06	5905.20
02118000	−80.659	35.845	0.0	87.1	11.0	317.4	6.5	7.1	49.1	37.0	0.11	0.41	1237.0	788.2	6.9	0.64	0.44	0.06	792.50
02143000	−81.403	35.684	0.0	75.4	23.0	445.2	13.0	5.9	76.6	12.2	0.03	0.05	1310.9	783.8	6.5	0.60	0.46	0.04	214.50
02143040	−81.567	35.591	0.0	75.0	21.4	547.8	15.7	2.6	90.2	3.9	0.01	0.02	1364.8	768.5	6.3	0.56	0.48	0.04	67.33
02143500	−81.264	35.422	0.0	88.5	9.7	289.5	3.8	8.6	39.2	46.0	0.15	0.58	1246.2	826.4	4.3	0.66	0.44	0.03	178.70
02192000	−82.770	33.974	0.0	91.0	6.6	217.7	4.3	7.7	53.3	22.7	0.59	3.60	1305.7	871.0	2.7	0.67	0.42	0.06	3703.68
02202500	−81.416	32.191	10.0	54.4	14.8	90.4	1.8	5.0	43.7	22.9	0.31	13.77	1206.0	957.9	0.4	0.79	0.33	0.03	6863.50
02217500	−83.423	33.947	0.0	95.1	4.9	269.6	4.8	15.8	45.1	26.0	0.60	3.19	1346.7	864.3	2.6	0.64	0.44	0.07	1030.81
02218500	−83.273	33.581	0.0	95.0	4.7	240.6	4.4	13.7	48.7	23.3	0.94	3.73	1309.9	879.3	2.4	0.67	0.41	0.07	2823.10
02219500	−83.349	33.609	0.0	96.9	2.7	226.6	3.4	9.0	45.8	27.3	0.96	5.30	1284.6	891.7	2.0	0.69	0.40	0.06	1129.20
02228000	−81.868	31.221	4.1	14.0	32.4	53.1	0.6	6.7	35.4	23.1	0.30	19.66	1264.7	1003.1	0.0	0.79	0.33	0.08	7226.10
02329000	−84.384	30.554	4.8	54.9	10.8	75.6	1.8	6.7	39.5	31.3	0.62	12.67	1366.7	1021.0	0.0	0.75	0.39	0.07	2952.60
02347500	−84.233	32.721	0.0	91.5	3.8	241.3	3.4	12.5	55.7	17.4	1.35	5.65	1281.6	903.2	1.2	0.70	0.39	0.09	4791.50

(*continued on next page*)

Appendix 1 (*continued*)

ID	Long	Lat	HGA	HGB	HGC	MEAN ELEV	SLOPE	URB	FST	AGR	OPEN WATER	WET LAND	MAP	PET	SDR	AI	RR	PSI	Area (km^2)
02349500	−84.044	32.298	8.9	73.6	11.3	208.4	3.4	9.3	55.4	17.7	1.00	7.08	1263.2	923.5	0.9	0.73	0.38	0.08	7511.00
03024000	−79.956	41.438	13.2	2.3	59.8	418.5	4.0	7.4	49.0	35.3	1.41	3.67	1152.0	603.7	24.4	0.52	0.41	0.10	2662.50
03032500	−79.394	40.994	1.2	13.8	73.5	474.4	9.4	8.8	64.8	22.7	0.44	0.37	1141.9	607.9	23.8	0.53	0.41	0.11	1367.50
03050500	−79.879	38.925	4.5	18.5	57.1	828.5	20.1	5.5	84.9	8.3	0.47	0.07	1346.0	597.2	23.3	0.44	0.54	0.08	704.50
03051000	−79.936	39.029	8.4	17.0	56.2	779.3	18.0	6.0	83.5	8.9	0.55	0.07	1332.8	604.0	22.4	0.45	0.53	0.08	1056.70
03054500	−80.040	39.150	9.7	11.0	65.1	712.4	16.6	6.2	82.9	9.4	0.53	0.04	1369.0	621.2	21.1	0.45	0.50	0.07	2372.40
03065000	−79.622	39.072	14.6	18.2	64.8	997.8	20.5	2.6	91.0	4.4	0.22	0.06	1364.6	570.9	24.3	0.42	0.52	0.07	893.60
03070000	−79.666	39.347	17.1	13.3	63.6	922.3	19.8	3.7	89.6	3.5	0.66	0.77	1385.5	584.5	24.0	0.42	0.52	0.07	2426.80
03075500	−79.426	39.422	17.1	9.8	67.9	794.8	9.8	7.9	65.7	22.8	0.50	1.11	1315.1	592.1	25.2	0.45	0.50	0.08	347.10
03109500	−80.541	40.676	1.2	16.8	65.8	346.3	6.0	12.9	45.4	38.0	0.97	0.62	983.6	655.6	19.7	0.67	0.37	0.12	1284.60
03111500	−80.734	40.193	0.0	19.3	77.7	342.7	8.9	10.0	54.6	30.2	0.93	0.19	1020.9	683.3	18.0	0.67	0.37	0.11	318.60
03114500	−80.997	39.475	0.0	8.9	53.2	314.3	17.6	4.5	88.3	6.6	0.23	0.00	1158.9	700.7	15.6	0.60	0.43	0.09	1186.20
03155500	−81.278	39.119	0.0	8.9	54.3	293.7	14.3	5.4	86.1	7.8	0.13	0.00	1145.7	709.5	14.9	0.62	0.43	0.08	1170.70
03159500	−82.088	39.329	0.0	36.9	55.1	274.3	7.3	9.5	58.7	29.6	0.66	0.12	1022.7	682.4	16.8	0.67	0.37	0.08	2442.40
03161000	−81.407	36.393	0.2	94.5	4.2	1023.7	17.0	9.6	66.8	19.8	0.09	0.12	1418.0	625.8	13.0	0.44	0.50	0.12	531.00
03167000	−80.887	36.939	0.8	47.2	44.1	765.6	12.0	7.1	50.8	41.6	0.04	0.06	1019.4	649.0	12.7	0.64	0.44	0.08	639.70
03168000	−80.746	36.937	0.5	74.0	21.9	869.0	14.3	6.3	61.2	30.4	0.27	0.09	1201.8	640.0	13.0	0.53	0.48	0.07	5703.20
031835000	−80.642	37.724	8.3	31.7	45.6	834.0	18.1	4.5	83.3	11.2	0.54	0.07	1152.1	619.1	20.3	0.54	0.48	0.06	3532.80
03184000	−80.805	37.640	7.7	31.7	48.0	804.5	17.9	4.7	82.2	12.1	0.56	0.06	1133.6	627.6	19.7	0.55	0.47	0.06	4193.20
03186500	−80.484	38.379	6.3	21.7	70.9	1074.7	22.4	1.9	97.0	0.3	0.21	0.02	1504.5	582.8	24.3	0.39	0.53	0.06	331.50
03281500	−83.677	37.479	0.0	61.8	27.2	366.3	22.2	5.9	83.6	4.6	0.31	0.00	1264.7	742.2	10.7	0.59	0.45	0.06	1870.00
03443000	−82.624	35.299	0.0	89.1	4.3	862.6	17.9	7.8	82.9	7.9	0.32	0.16	1877.7	694.4	6.9	0.37	0.64	0.04	766.60
03504000	−83.619	35.127	0.0	99.1	0.0	1211.9	26.9	1.9	97.0	0.3	0.02	0.15	2072.0	626.1	12.6	0.30	0.57	0.09	134.40
03512000	−83.354	35.461	0.5	95.2	3.3	1147.9	34.0	3.8	94.0	1.4	0.00	0.04	1655.4	611.1	13.6	0.37	0.54	0.06	476.60
03524000	−82.155	36.945	0.1	61.6	36.1	760.9	18.3	8.0	57.9	30.8	0.08	0.01	1159.1	662.0	13.6	0.57	0.45	0.08	1367.50
03531500	−83.095	36.662	0.0	47.5	48.6	658.9	21.8	8.3	71.9	4.0	0.20	0.00	1383.8	703.2	12.4	0.51	0.50	0.08	826.20
03550000	−83.981	35.139	0.2	87.0	9.6	762.5	24.2	6.6	87.1	5.4	0.05	0.24	1756.7	687.3	10.9	0.39	0.54	0.10	269.40
04221000	−75.139	42.166	3.3	2.4	90.6	629.8	10.9	3.6	54.3	36.7	0.07	0.08	998.1	558.7	27.5	0.56	0.38	0.13	745.90
04256000	−76.912	41.325	34.3	2.1	45.9	497.3	5.1	0.0	64.6	0.0	1.93	23.19	1242.0	526.8	37.2	0.42	0.62	0.08	238.28

AGR, percentage of agricultural areas in each catchment (%); AI, Aridity Index (%); FST, percentage of forest areas in each catchment (%); Long, Longitude (°); Lat, Latitude (°); MAP, Mean Annual Precipitation (mm); MEAN ELEV, catchments mean elevation (m); OPEN WATER, percentage of open water per catchment (%); PET, potential evapotranspiration (mm); PSI, precipitation seasonality index; RR, runoff ratio (%); SDR, snow day ratio (%); SLOPE, catchments slope in (%); URB, percentage of urban areas in each catchment (%); WET LAND, percentage of wet land per catchment (%).

References

Ameli, A.A., Craig, J.R., McDonnell, J.J., 2015. Are all runoff processes the same? Numerical experiments comparing a Darcy-Richards solver to an overland flow-based approach for subsurface storm runoff simulation. Water Resour. Res. 51 (12), 10008–10028.

Arora, M., Goel, N.K., Singh, P., Singh, R.D., 2005. Regional flow duration curve for a Himalayan river Chenab. Hydrol. Res. 36 (2), 193–206.

Bathurst, J.C., 2014. Comment on A paradigm shift in understanding and quantifying the effects of forest harvesting on floods in snow environments. Water Resour. Res. 50 (3), 2756–2758. by KC Green and Y Alila.

Berghuijs, W.R., Sivapalan, M., Woods, R.A., Savenije, H.H., 2014. Patterns of similarity of seasonal water balances: a window into streamflow variability over a range of time scales. Water Resour. Res. 50 (7), 5638–5661.

Berghuijs, W.R., Woods, R.A., Hutton, C.J., Sivapalan, M., 2016. Dominant flood generating mechanisms across the United States. Geophys. Res. Lett. 43 (9), 4382–4390.

Beven, K., Germann, P., 1982. Macropores and water flow in soils. Water Resour. Res. 18 (5), 1311–1325.

Beven, K., Wood, E.F., 1983. Catchment geomorphology and the dynamics of runoff contributing areas. J. Hydrol. 65 (1), 139–158.

Beven, K.J., Kirkby, M.J., 1979. A physically based, variable contributing area model of basin hydrology/Un modèle à base physique de zone d'appel variable de l'hydrologie du bassin versant. Hydrol. Sci. J. 24 (1), 43–69. https://doi.org/10.1080/02626667909491834.

Birkinshaw, S.J., Bathurst, J.C., Iroumé, A., Palacios, H., 2011. The effect of forest cover on peak flow and sediment discharge—an integrated field and modelling study in central–southern Chile. Hydrol. Process. 25 (8), 1284–1297.

Bonell, M., 1993. Progress in the understanding of runoff generation dynamics in forests. J. Hydrol. 150 (2–4), 217–275.

Botter, G., Porporato, A., Daly, E., Rodriguez-Iturbe, I., Rinaldo, A., 2007a. Probabilistic characterization of base flows in river basins: roles of soil, vegetation, and geomorphology. Water Resour. Res. 43 (6), W06404. https://doi.org/10.1029/2006WR005397.

Botter, G., Peratoner, F., Porporato, A., Rodriguez-Iturbe, I., Rinaldo, A., 2007b. Signatures of large-scale soil moisture dynamics on streamflow statistics across US climate regimes. Water Resour. Res. 43 (11), W11413. https://doi.org/10.1029/2007WR006162.

Botter, G., Porporato, A., Rodriguez-Iturbe, I., Rinaldo, A., 2009. Nonlinear storage-discharge relations and catchment streamflow regimes. Water Resour. Res. 45 (10), W10427. https://doi.org/10.1029/2008WR007658.

Botter, G., 2010. Stochastic recession rates and the probabilistic structure of stream flows. Water Res. Res. 46 (12), W12527. https://doi.org/10.1029/2010WR009217.

Burnash, R.J.C., 1995. The NWS river forecast system—catchment modeling. In: Singh, V.P. (Ed.), Computer Models of Watershed Hydrology. Water Resources Publications, LittletonCO, pp. 311–366.

Burt, T.P., Swank, W.T., 1992. Flow frequency responses to hardwood-to-grass conversion and subsequent succession. Hydrol. Process. 6 (2), 179–188.

Butt, T., Russell, P., Turner, I., 2001. The influence of swash infiltration–exfiltration on beach face sediment transport: onshore or offshore? Coast. Eng. 42 (1), 35–52.

Castellarin, A., Vogel, R.M., Brath, A., 2004a. A stochastic index flow model of flow duration curves. Water Resour. Res. 40 (3), W03104. https://doi.org/10.1029/2003WR002524.

Castellarin, A., Galeati, G., Brandimarte, L., Montanari, A., Brath, A., 2004b. Regional flow-duration curves: reliability for ungauged basins. Adv. Water Resour. 27 (10), 953–965.

Ceola, S., Botter, G., Bertuzzo, E., Porporato, A., Rodriguez-Iturbe, I., Rinaldo, A., 2010. Comparative study of ecohydrological streamflow probability distributions. Water Resour. Res. 46 (9), W09502. https://doi.org/10.1029/2010WR009102.

Cheng, L., Yaeger, M., Viglione, A., Coopersmith, E., Ye, S., Sivapalan, M., 2012. Exploring the physical controls of regional patterns of flow duration curves–Part 1: insights from statistical analyses. Hydrol. Earth Syst. Sci. 16 (11), 4435–4446.

Cigizoglu, H.K., Bayazit, M., 2000. A generalized seasonal model for flow duration curve. Hydrol. Process. 14 (6), 1053–1067.

Claps, P., Fiorentino, M., 1997. Probabilistic flow duration curves for use in environmental planning and management. Integrated approach to environmental data management systems, NATO-ASI series, 2(31), pp. 255–266.

Coopersmith, E., Yaeger, M.A., Ye, S., Cheng, L., Sivapalan, M., 2012. Exploring the physical controls of regional patterns of flow duration curves–Part 3: a catchment classification system based on regime curve indicators. Hydrol. Earth Syst. Sci. 16 (11), 4467–4482. https://doi.org/10.1029/2010WR009286.

Crooks, S., Davies, H., 2001. Assessment of land use change in the Thames catchment and its effect on the flood regime of the river. Phys. Chem. Earth, Part B Hydrol. Ocean. Atmosph. 26 (7–8), 583–591.

Croker, K.M., Young, A.R., Zaidman, M.D., Rees, H.G., 2003. Flow duration curve estimation in ephemeral catchments in Portugal. Hydrol. Sci. J. 48 (3), 427–439.

Di Matteo, L., Dragoni, W., Maccari, D., Piacentini, S.M., 2017. Climate change, water supply and environmental problems of headwaters: The paradigmatic case of the Tiber, Savio and Marecchia rivers (Central Italy). Sci. Tot. Environ. 598, 733–748.

Dodd, M.B., Lauenroth, W.K., 1997. The influence of soil texture on the soil water dynamics and vegetation structure of a shortgrass steppe ecosystem. Plant Ecol. 133 (1), 13–28.

Duan, Q., Schaake, J., Andreassian, V., Franks, S., Goteti, G., Gupta, H.V., Gusev, Y.M., Habets, F., Hall, A., Hay, L., Hogue, T., 2006. Model Parameter Estimation Experiment (MOPEX): An overview of science strategy and major results from the second and third workshops. J. Hydrol. 320 (1), 3–17.

Eisenlohr, W. S., 1952. Floods of July 18, 1942 in north-central Pennsylvania, U.S. Geological Survey. Water Supply Paper, 1134-B, pp. 100.

Erskine, H.M., 1951. Flood of August 4-5, 1943, in central West Virginia, with a summary of flood stages and discharges in West Virginia (No. 1134-A). USGPO. http://pubs.er.usgs.gov/publication/wsp1134A.

Fenicia, F., Savenije, H.H., Matgen, P., Pfister, L., 2008. Understanding catchment behavior through stepwise model concept improvement. Water Resour. Res. 44 (1), W01402. https://doi.org/10.1029/2006WR005563.

Fennessey, N., Vogel, R.M., 1990. Regional flow-duration curves for ungauged sites in Massachusetts. J. Water Resour. Plann. Manage. 116 (4), 530–549.

Fovell, R.G., Fovell, M.Y.C., 1993. Climate zones of the conterminous United States defined using cluster analysis. J. Clim. 6 (11), 2103–2135.

Gan, T.Y., Burges, S.J., 2006. Assessment of soil-based and calibrated parameters of the Sacramento model and parameter transferability. J. Hydrol. 320 (1), 117–131.

Gao, H., Hrachowitz, M., Schymanski, S.J., Fenicia, F., Sriwongsitanon, N., Savenije, H. H.G., 2014. Climate controls how ecosystems size the root zone storage capacity at catchment scale. Geophys. Res. Lett. 41 (22), 7916–7923.

Graham, C.B., Woods, R.A., McDonnell, J.J., 2010. Hillslope threshold response to rainfall:(1) A field based forensic approach. J. Hydrol. 393 (1), 65–76.

Guebert, M.D., Gardner, T.W., 2001. Macropore flow on a reclaimed surface mine: infiltration and hillslope hydrology. Geomorphology 39 (3), 151–169.

Huff, F.A., 1967. Time distribution of rainfall in heavy storms. Water Resour. Res. 3 (4), 1007–1019.

Hentati, A., Kawamura, A., Amaguchi, H., Iseri, Y., 2010. Evaluation of sedimentation vulnerability at small hillside reservoirs in the semi-arid region of Tunisia using the Self-Organizing Map. Geomorphology 122 (1), 56–64.

Hershfield D.M., 1961. Rainfall frequency atlas of the United States for durations from 30 minutes to 24 hours and return periods from 1 to 100 years. US Department of Commerce, Weather Bureau. Washington D.C., Technical Report No. 40.

Hewlett, J.D., Hibbert, A.R., 1967. Factors affecting the response of small watersheds to precipitation in humid areas. Forest Hydrol. 1, 275–290.

Hicks, N.S., Smith, J.A., Miller, A.J., Nelson, P.A., 2005. Catastrophic flooding from an orographic thunderstorm in the central Appalachians. Water Resour. Res. 41 (12), W12428.

Hrachowitz, M., Savenije, H.H.G., Blöschl, G., McDonnell, J.J., Sivapalan, M., Pomeroy, J.W., Arheimer, B., Blume, T., Clark, M.P., Ehret, U., Fenicia, F., 2013. A decade of Predictions in Ungauged Basins (PUB)—a review. Hydrol. Sci. J. 58 (6), 1198–1255.

Iacobellis, V., 2008. Probabilistic model for the estimation of T year flow duration curves. Water Resour. Res. 44 (2), W02413. https://doi.org/10.1029/2006WR005400.

Kelson, K.I., Wells, S.G., 1989. Geologic influences on fluvial hydrology and bedload transport in small mountainous watersheds, northern New Mexico USA. Earth Surf. Process. Landfor. 14 (8), 671–690.

Koutsoyiannis, D., Foufoula-Georgiou, E., 1993. A scaling model of a storm hyetograph. Water Resour. Res. 29 (7), 2345–2361.

Koren, V., Smith, M., Duan, Q., 2003. Use of a priori parameter estimates in the derivation of spatially consistent parameter sets of rainfall-runoff models doi:. In: Duan, Q., Gupta, H.V., Sorooshian, S., Rousseau, A.N., Turcotte, R. (Eds.), Calibration of Watershed Models. American Geophysical Union, Washington, D. C. 10.1002/9781118665671.ch18.

LeBoutillier, D.W., Waylen, P.R., 1993. Regional variations in flow-duration curves for rivers in British Columbia. Can. Phys. Geogr. 14 (4), 359–378.

McDonnell, J.J., 1990. A rationale for old water discharge through macropores in a steep, humid catchment. Water Resour. Res. 26 (11), 2821–2832.

Milly, P.C., Betancourt, J., Falkenmark, M., Hirsch, R.M., Kundzewicz, Z.W., Lettenmaier, D.P., Stouffer, R.J., 2008. Stationarity is dead: Whither water management? Science 319 (5863), 573–574.

Muneepeerakul, R., Azaele, S., Botter, G., Rinaldo, A., Rodriguez-Iturbe, I., 2010a. Daily streamflow analysis based on a two-scaled gamma pulse model. Water Resour. Res. 46 (11).

Musiake, K., Inokuti, S., Takahasi, Y., 1975. Dependence of low flow characteristics on basin geology in mountainous areas of Japan. IAHS Publication, pp. 147–156.

Miller, A.J., 1990. Flood hydrology and geomorphic effectiveness in the central Appalachians. Earth Surf. Process. Landf. 15 (2), 119–134.
Muneepeerakul, R., Azaele, S., Botter, G., Rinaldo, A., Rodriguez-Iturbe, I., 2010b. Daily streamflow analysis based on a two-scaled gamma pulse model. Water Resour. Res. 46 (11), W11546.
Nash, J.E., Sutcliffe, J.V., 1970. River flow forecasting through conceptual models part I—A discussion of principles. J. Hydrol. 10 (3), 282–290.
Newman, A.J., Clark, M.P., Sampson, K., Wood, A., Hay, L.E., Bock, A., Viger, R.J., Blodgett, D., Brekke, L., Arnold, J.R., Hopson, T., 2015. Development of a large-sample watershed-scale hydrometeorological data set for the contiguous USA: data set characteristics and assessment of regional variability in hydrologic model performance. Hydrol. Earth Syst. Sci. 19 (1), 209–223.
Perry, C.A., Combs, L.J., 1998. Summary of floods in the United States, January 1992 through September 1993. US Geological Survey water-supply paper vol. 2499, pp. 1–286.
Perry, C.A., Aldridge, B.N., Ross, H.C., 2001. Summary of significant floods in the United States, Puerto Rico, and the Virgin Islands, 1970 through 1989. US Government Printing Office.
Price, K., 2011. Effects of watershed topography, soils, land use, and climate on baseflow hydrology in humid regions: a review. Progr. Phys. Geogr. 35 (4), 465–492.
Reynard, N.S., Prudhomme, C., Crooks, S.M., 2001. The flood characteristics of large UK rivers: potential effects of changing climate and land use. Clim. Change 48 (2), 343–359.
Robinson, J.S., Sivapalan, M., 1997. Temporal scales and hydrological regimes: Implications for flood frequency scaling. Water Resour. Res. 33 (12), 2981–2999.
Rousseau, A.N., Hentati, A., Tremblay, S., Quilbé, R., Villeneuve, J.P., 2005. Computation of the topographic index on 16 watersheds in Quebec (No. R800f). INRS, Centre Eau, Terre et Environnement.
Rice, K.C., Hornberger, G.M., 1998. Comparison of hydrochemical tracers to estimate source contributions to peak flow in a small, forested, headwater catchment. Water Resour. Res. 34 (7), 1755–1766.
Sawicz, K., Wagener, T., Sivapalan, M., Troch, P.A., Carrillo, G., 2011. Catchment classification: empirical analysis of hydrologic similarity based on catchment function in the eastern USA. Hydrol. Earth Syst. Sci. 15 (9), 2895–2911.
Schaake, J., Franz, K., Bradley, A., Buizza, R., 2006. The hydrologic ensemble prediction experiment (HEPEX). Hydrol. Earth Syst. Sci. Discuss. 3 (5), 3321–3332.
Sefton, C.E.M., Howarth, S.M., 1998. Relationships between dynamic response characteristics and physical descriptors of catchments in England and Wales. J. Hydrol. 211 (1), 1–16.
Singh, R.D., Mishra, S.K., Chowdhary, H., 2001. Regional flow-duration models for large number of ungauged Himalayan catchments for planning microhydro projects. J. Hydrol. Eng. 6 (4), 310–316.
Sivapalan, M., Samuel, J.M., 2009. Transcending limitations of stationarity and the return period: process-based approach to flood estimation and risk assessment. Hydrol. Process. 23 (11), 1671–1675.
Sklash, M.G., Farvolden, R.N., 1979. The role of groundwater in storm runoff. Dev. Water Sci. 12, 45–65.
Smakhtin, V.Y., Hughes, D.A., Creuse-Naudin, E., 1997. Regionalization of daily flow characteristics in part of the Eastern Cape South Africa. Hydrol. Sci. J. 42 (6), 919–936.
Smakhtin, V.Y., Masse, B., 2000. Continuous daily hydrograph simulation using duration curves of a precipitation index. Hydrol. Process. 14, 1083–1100.
Smith, J.A., Baeck, M.L., Steiner, M., Miller, A.J., 1996. Catastrophic rainfall from an upslope thunderstorm in the central Appalachians: The Rapidan storm of June 27, 1995. Water Resour. Res. 32 (10), 3099–3113.
Sorooshian, S., Duan, Q., Gupta, V.K., 1993. Calibration of rainfall-runoff models: application of global optimization to the sacramento soil moisture accounting model. Water Resour. Res. 29 (4), 1185–1194.
Sugiyama, H., Vudhivanich, V., Whitaker, A.C., Lorsirirat, K., 2003. Stochastic flow duration curves for evaluation of flow regimes in rivers. JAWRA 39 (1), 47–58.
Swift Jr., L.W., Cunningham, G.B., Douglass, J.E., 1988. Climatology and hydrology. Forest hydrology and ecology at Coweeta. Springer, New York, pp. 35–55.
van Werkhoven, K., Wagener, T., Reed, P., Tang, Y., 2008. Characterization of watershed model behavior across a hydroclimatic gradient. Water Resour. Res. 44 (1), W01429. https://doi.org/10.1029/2007WR006271.
Verdon-Kidd, D.C., Kiem, A.S., 2009. On the relationship between large-scale climate modes and regional synoptic patterns that drive Victorian rainfall. Hydrol. Earth Syst. Sci. 13 (4), 467–479.
Vogel, R.M., Fennessey, N.M., 1994. Flow-duration curves. I: new interpretation and confidence intervals. J. Water Resour. Plann. Manage. 120 (4), 485–504.
Vogel, R.M., Fennessey, N.M., 1995. Flow duration curves II: a review of applications in water resources planning. JAWRA 31 (6), 1029–1039.
Ward, R.C., Robinson, M., 1990. Principles of Hydrology. McGraw-Hill, Maidenhead, Berkshire, England.
Weiler, M., McDonnell, J.J., 2007. Conceptualizing lateral preferential flow and flow networks and simulating the effects on gauged and ungauged hillslopes. Water Resour. Res. 43 (3), W03403. https://doi.org/10.1029/2006WR004867.
Wood, M.K., Blackburn, W.H., 1984. An evaluation of the hydrologic soil groups as used in the SCS runoff method on rangelands. JAWRA 20 (3), 379–389.
Yadav, M., Wagener, T., Gupta, H., 2007. Regionalization of constraints on expected watershed response behavior for improved predictions in ungauged basins. Adv. Water Res. 30 (8), 1756–1774.
Yaeger, M., Coopersmith, E., Ye, S., Cheng, L., Viglione, A., Sivapalan, M., 2012. Exploring the physical controls of regional patterns of flow duration curves–Part 4: a synthesis of empirical analysis, process modeling and catchment classification. Hydrol. Earth Syst. Sci. 16 (11), 4483–4498.
Yeakley, J.A., Swank, W.T., Swift, L.W., Hornberger, G.M., Shugart, H.H., 1998. Soil moisture gradients and controls on a southern Appalachian hillslope from drought through recharge. Hydrol. Earth Syst. Sci. 2 (1), 41–49.
Ye, S., Yaeger, M., Coopersmith, E., Cheng, L., Sivapalan, M., 2012. Exploring the physical controls of regional patterns of flow duration curves–Part 2: Role of seasonality, the regime curve, and associated process controls. Hydrol. Earth Syst. Sci. 16 (11), 4447–4465.
Yokoo, Y., Sivapalan, M., 2011. Towards reconstruction of the flow duration curve: development of a conceptual framework with a physical basis. Hydrol. Earth Syst. Sci. 15 (9), 2805–2819.
Zhao, R.J., Liu, X.R., 1995. The Xinanjiang Model. In: Singh, V.P. (Ed.), Computer Models of Watershed Hydrology. Water Resources Publication, US, pp. 215–232.
Zhang, Z., Wagener, T., Reed, P., Bhushan, R., 2008. Reducing uncertainty in predictions in ungauged basins by combining hydrologic indices regionalization and multiobjective optimization. Water Resour. Res. 44 (12). W00B04.